

A Statistical Mechanics Perspective on Glasses and Aging

Ludovic Berthier¹ and Giulio Biroli²

¹*Laboratoire des Colloïdes, Verres et Nanomatériaux,
Université Montpellier II and CNRS, 34095 Montpellier, France*

²*Service de Physique Théorique Orme des Merisiers – CEA Saclay, 91191 Gif sur Yvette Cedex, France*
(Dated: December 4, 2007)

We briefly review the field of the glass transition, glassy dynamics and aging from a statistical mechanics perspective. We give a broad introduction to the subject and then explain the main phenomenology and puzzles encountered in glassy systems. We discuss the important role played by computer simulations to understand the dynamics of systems close to the glass transition at the molecular level. We discuss more particularly the idea of a spatially heterogeneous dynamics that characterizes the relaxation of supercooled liquids. We review the main theoretical approaches that are currently available to account for these glassy phenomena and discuss the physics of aging and off-equilibrium dynamics exhibited by glassy materials. We conclude the review by giving some perspectives for future research in the field.

Contents

I. Glossary	1
II. Glasses and aging: a broad introduction	2
III. Phenomenology	3
IV. Taxonomy of ‘glasses’ in science	6
A. The jamming transition of colloids and grains	6
B. Other ‘glasses’ in physics and beyond	7
V. Numerical simulations	7
VI. Dynamic heterogeneity	9
A. Existence of spatio-temporal dynamic fluctuations	9
B. Multi-point correlation functions	11
VII. Some theory and models	13
A. Cooperativity, chaotic energy landscapes and Random First Order Theory	13
B. Free volume, defects, and facilitated models	16
C. Geometric frustration, avoided criticality, and Coulomb frustrated theories	19
VIII. Aging and off-equilibrium	20
A. Why aging?	20
B. Memory and rejuvenation effects	21
C. Mean-field aging and effective temperatures	22
D. Beyond mean-field	23
E. Driven glassy materials	25
IX. Future directions	26
Acknowledgments	26
References	26

I. GLOSSARY

In this preliminary section, we give a few concise definitions of the most important concepts discussed in this article.

Glass transition—For molecular liquids, the glass transition denotes a crossover from a viscous liquid to an amorphous solid. Experimentally, the crossover takes place at the glass temperature, T_g , conventionally defined as the temperature where the liquid’s viscosity reaches the arbitrary value of 10^{12} Pa.s. The glass transition more generally applies to many different condensed matter systems where a crossover or, less frequently, a true phase transition, takes place between an ergodic phase and a frozen, amorphous glassy phase.

Aging—In the glass phase, disordered materials are characterized by relaxation times that exceed common observation timescales, so that a material quenched in its glass phase never reaches equilibrium (neither a metastable equilibrium). It exhibits instead an aging behaviour during which its physical properties keep evolving with time.

Dynamic heterogeneity—Relaxation spectra in supercooled liquids are very broad. This is associated to a spatial distribution of timescales: at any given time, different regions in the liquid relax at different rates. Since the supercooled liquid is ergodic, slow regions eventually become fast, and vice versa. Dynamic heterogeneity refers to the existence of these non-trivial spatio-temporal fluctuations in the local dynamical behaviour, a phenomenon observed in virtually all disordered systems with slow dynamics.

Effective temperature—An aging material relaxes very slowly, trying (in vain) to reach its equilibrium state. During this process, the system probes states that do not correspond to thermodynamic equilibrium, so that its thermodynamic properties can not be rigorously defined. Any practical measurement of its temperature becomes a frequency-dependent operation. A ‘slow’ thermometer tuned to the relaxation timescale of the aging system

measures an effective temperature corresponding to the ratio between spontaneous fluctuations (correlation) and linear response (susceptibility). This corresponds to a generalized form of the fluctuation-dissipation theorem for off-equilibrium materials.

Frustration—Impossibility of simultaneously minimizing all the interaction terms in the energy function of the system. Frustration might arise from quenched disorder (as in the spin glass models), from competing interactions (as in geometrically frustrated magnets), or from competition between a ‘locally preferred order’, and global, e.g. geometric, constraints (as in hard spheres packing problems).

II. GLASSES AND AGING: A BROAD INTRODUCTION

Glasses belong to a well-known state of matter: we easily design glasses with desired mechanical or optical properties on an industrial scale, they are widely present in our daily life. Yet, a deep microscopic understanding of the glassy state of matter remains a challenge for condensed matter physicists [1, 2]. Glasses share similarities with crystalline solids (they are both mechanically rigid), but also with liquids (they both have similar disordered structures at the molecular level). It is mainly this mixed character that makes them fascinating even to non-scientists.

A glass can be obtained by cooling the temperature of a liquid below its glass temperature, T_g . The quench must be fast enough such that the more standard first order phase transition towards the crystalline phase is avoided. The glass ‘transition’ is not a thermodynamic transition at all, since T_g is only empirically defined as the temperature below which the material has become too viscous to flow on a ‘reasonable’ timescale (and it is hard to define the word ‘reasonable’ in any reasonable manner). Therefore, T_g does not play a fundamental role, as a phase transition temperature would. It is simply the temperature below the material looks solid. When quenched in the glass phase below T_g , liquids slowly evolve towards an equilibrium state they cannot reach on experimental timescales. Physical properties are then found to evolve slowly with time in far from equilibrium states, a process known as ‘aging’ [3].

Describing theoretically and quantifying experimentally the physical mechanisms responsible for the viscosity increase of liquids approaching the glass transition and for aging phenomena below the glass transition certainly stand as central open challenges in condensed matter physics. Since statistical mechanics aims at understanding the collective behaviour of large assemblies of interacting objects, it comes as no surprise that it is a central tool in this field. We shall therefore summarize the understanding gained from statistical mechanics perspectives into the problem of glasses and aging.

The subject has quite broad implications. A material

is said to be ‘glassy’ when its typical relaxation timescale becomes of the order of, and often much larger than, the typical duration of an experiment or a numerical simulation. With this generic definition, a large number of systems can be considered as glassy materials [4]. One can be interested in the physics of liquids (window glasses are then the archetype), in ‘hard’ condensed matter systems (for instance type II superconductors in the presence of disorder such as high- T_c superconducting materials), in charge density waves or spin glasses, in ‘soft’ condensed matter with numerous complex fluids such as colloidal assemblies, emulsions, foams, but also granular materials, proteins, etc. All these materials exhibit, in some part of their phase diagrams, some sort of glassy dynamics characterized by a very rich phenomenology with effects such as aging, hysteresis, creep, memory, effective temperatures, rejuvenation, dynamic heterogeneity, non-linear response, etc.

These long lists explain why this area of research has received increasing attention from physicists in the last two decades. ‘Glassy’ topics now go much beyond the physics of simple liquids (glass transition physics) and models and concepts developed for one system often find applications elsewhere in physics, from algorithmic to biophysics [5]. Motivations to study glassy materials are numerous. Glassy materials are everywhere around us and therefore obviously attract interest beyond academic research. At the same time, the glass conundrum provides theoretical physicists with deep fundamental questions since classical concepts and tools are sometimes not sufficient to properly account for the glass state. Moreover, simulating in the computer the dynamics of microscopically realistic material on timescales that are experimentally relevant is not an easy task, even with modern computers.

Studies on glassy materials constitute an exciting research area where experiments, simulations and theoretical calculations can meet, where both applied and fundamental problems are considered. How can one observe, understand, and theoretically describe the rich phenomenology of glassy materials? What are the fundamental quantities and concepts that emerge from these descriptions?

In the following, we first discuss in Sec. III the phenomenology of glass-forming liquids. In Sec. IV we briefly present other type of glasses in particular colloids and granular materials. We then describe how computer simulations have provided deep insights into the glass problem in Sec. V. We discuss more particularly the issue of dynamic heterogeneity in Sec. VI. We briefly summarize some of the main theoretical perspectives currently available in the field in Sec. VII. We discuss aging and off-equilibrium phenomena in Sec. VIII. Finally we discuss issues that seem important for future research in Sec. IX.

III. PHENOMENOLOGY

A vast majority of liquids (molecular liquids, polymeric liquids, etc.) form a glass if cooled fast enough in order to avoid the crystallisation transition [1]. Typical values of cooling rate in laboratory experiments are 0.1 – 100 K/min. The metastable phase reached in this way is called ‘supercooled phase’. In this regime the typical timescales increase in a dramatic way and they end up to be many orders of magnitudes larger than microscopic timescales at T_g , the glass transition temperature.

For example, around the melting temperature T_m , the typical timescale τ_α on which density fluctuations relax, is of the order of $\sqrt{ma^2/K_B T}$, which corresponds to few picoseconds (m is the molecular mass, T the temperature, K_B the Boltzmann constant and a a typical distance between molecules). At T_g , which as a rule of thumb is about $\frac{2}{3}T_m$, the typical timescale has become of the order of 100 s, i.e. 14 orders of magnitude larger! This phenomenon is accompanied by a concomitant increase of the shear viscosity η . This can be understood by a simple Maxwell model in which η and τ are related by $\eta = G_\infty \tau_\alpha$, where G_∞ is the instantaneous (elastic) shear modulus which does not vary considerably in the supercooled regime. In fact, viscosities at the glass transition temperature are of the order of 10^{12} Pa.s. In order to grasp how huge this value is, recall that the typical viscosity of water at ambient temperature is of the order of 10^{-2} Pa.s. How long would one have to wait to drink a glass of water with a viscosity 10^{14} times larger?

As a matter of fact, the temperature at which a liquid does not flow anymore and becomes an amorphous solid, called a ‘glass’, is protocol dependent. It depends on the cooling rate and on the patience of the people carrying out the experiment: solidity is a timescale dependent notion. Pragmatically, T_g is defined as the temperature at which the shear viscosity is equal to 10^{13} Poise (also 10^{12} Pa.s).

The increase of the relaxation timescale of supercooled liquids is remarkable not only because of the large number of decades involved but also because of its temperature dependence. This is vividly demonstrated by plotting the logarithm of the viscosity (or the relaxation time) as a function of T_g/T , as in Fig. 1. This is called the ‘Angell’ plot [1] and is very helpful in classifying supercooled liquids. A liquid is called strong or fragile depending on its position in the Angell plot. Straight lines correspond to ‘strong’ glass-formers and to an Arrhenius behaviour. In this case, one can extract from the plot an effective activation energy, suggesting a quite simple mechanism for relaxation that consists in ‘breaking’ locally a chemical bond. The typical relaxation time is then dominated by the energy barrier to activate this process and, hence, has an Arrhenius behaviour. Window glasses fall in this category [177]. If one tries to define an effective activation energy for fragile glass-formers using the slope of the curve in Fig. 1, then one finds that this energy scale increases when the temperature decreases,

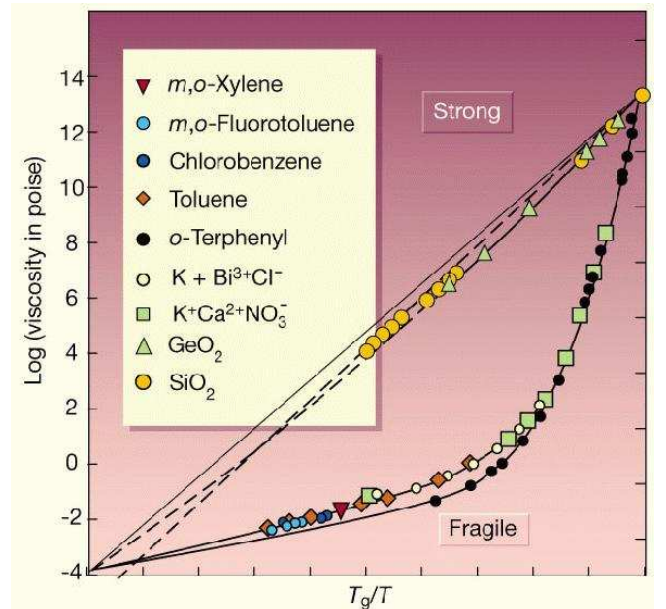


FIG. 1: Angell plot of the viscosity of several glass-forming liquids approaching the glass temperature T_g [2]. For ‘strong’ glasses, the viscosity increases in an Arrhenius manner as temperature is decreased, $\log \eta \sim E/(K_B T)$, where E is an activation energy and the plot is a straight line, as for silica. For ‘fragile’ liquids, the plot is bent and the effective activation energy increases when T is decreased towards T_g , as for ortho-terphenyl.

a ‘super-Arrhenius’ behaviour. This increase of energy barriers immediately suggests that the glass formation is a collective phenomenon for fragile supercooled liquids. Support for this interpretation is provided by the fact that a good fit of the relaxation time or the viscosity is given by the Vogel-Fulcher-Tamman law (VFT):

$$\tau_\alpha = \tau_0 \exp \left[\frac{DT_0}{(T - T_0)} \right], \quad (1)$$

which suggests a divergence of the relaxation time, and therefore a phase transition of some kind, at a finite temperature T_0 . A smaller D in the VFT law corresponds to a more fragile glass. Note that there are other comparably good fits of these curves, such as the Bässler law [6],

$$\tau_\alpha = \tau_0 \exp \left(K \left(\frac{T_*}{T} \right)^2 \right), \quad (2)$$

that only lead to a divergence at zero temperature. Actually, although the relaxation time increases by 14 orders of magnitude, the increase of its logarithm, and therefore of the effective activation energy is very modest, and experimental data do not allow one to unambiguously determine the true underlying functional law without any reasonable doubt. For this and other reasons, physical interpretations in terms of a finite temperature phase transition must always be taken with a grain of salt.

Substance	o-terphenyl	2-methyltetra-hydrofuran	n-propanol	3-bromopentane
T_g	246	91	97	108
T_0	202.4	69.6	70.2	82.9
T_K	204.2	69.3	72.2	82.5
T_K/T_0	1.009	0.996	1.028	0.995

TABLE I: Values of glass transition temperature, VFT singularity and Kauzmann temperatures for four supercooled liquids [7].

However, there are other experimental facts that shed some light and reinforce this interpretation. Among them, is an empirical connection found between kinetic and thermodynamic behaviours. Consider the part of the entropy of the liquids, S_{exc} , which is in excess compared to the entropy of the corresponding crystal. Once this quantity, normalized by its value at the melting temperature, is plotted as a function of T , a remarkable connection with the dynamics emerges. As for the relaxation time one cannot follow this curve below T_g in thermal equilibrium. However, extrapolating the curve below T_g apparently indicates that the excess entropy vanishes at some finite temperature, called T_K , which is very close to zero for strong glasses and, generically, very close to T_0 , the temperature at which a VFT fit diverges. This coincidence is quite remarkable: for materials with glass transition temperatures that vary from 50 K to 1000 K the ratio T_K/T_0 remains close to 1, up to a few percents. Examples reported in Ref. [7] are provided in Table I.

The chosen subscript for T_K stands for Kauzmann [8] which recognized T_K as a very important temperature in the glass phase diagram. Kauzmann further claimed that some change of behaviour (phase transition, crystal nucleation, etc.) must take place above T_K , because below T_K the entropy of the liquid, a disordered state of matter, becomes less than the entropy of the crystal, an ordered state of matter. This situation that seemed paradoxical at that time is not a serious problem. There is no general principle that would constraint the entropy of the liquid to be larger than that of the crystal. As a matter of fact, the crystallisation transition for hard spheres takes place precisely because the crystal becomes the state with the largest entropy at sufficiently high density.

On the other hand, the importance of T_K stands, partially because it is experimentally very close to T_0 . Additionally, the quantity S_{exc} which vanishes at T_K , is thought to be a proxy for the so-called configurational entropy, S_c , which quantifies the number of metastable states. A popular physical picture due to Goldstein [9] is that close to T_g the system explores a part of the energy landscape (or configuration space) which is full of minima separated by barriers that increase when temperature decreases. The dynamic evolution in the energy landscape would then consist in a rather short equilibration inside the minima followed by ‘jumps’ between different minima. At T_g the barriers have become so large that the system remains trapped in one minimum, identified as one of the possible microscopic amorphous

configurations of a glass. Following this interpretation, one can split the entropy into two parts. A first contribution is due to the fast relaxation inside one minimum, a second counts the number of metastable states, $S_c = \log N_{\text{metastable}}$, which is called the ‘configurational’ entropy. Assuming that the contribution to the entropy due to the ‘vibrations’ around an amorphous glass configuration is not very different from the entropy of the crystal, one finds that $S_{\text{exc}} \approx S_c$. In that case, T_K would correspond to a temperature at which the configurational entropy vanishes. This in turn would lead to a discontinuity (a downward jump) of the specific heat and would truly correspond to a thermodynamic phase transition.

At this point the reader might have reached the conclusion that the glass transition may not be such a difficult problem: there are experimental indications of a diverging timescale and a concomitantly singularity in the thermodynamics. It simply remains to find static correlation functions displaying a diverging correlation length related to the emergence of ‘amorphous order’, which would indeed classify the glass transition as a standard second order phase transition. Remarkably, this remains an open and debated question despite several decades of research. Simple static correlation function are quite featureless in the supercooled regime, notwithstanding the dramatic changes in the dynamics. A simple static quantity is the structure factor defined by

$$S(q) = \left\langle \frac{1}{N} \delta\rho_{\mathbf{q}} \delta\rho_{-\mathbf{q}} \right\rangle, \quad (3)$$

where the Fourier component of the density reads

$$\delta\rho_{\mathbf{q}} = \sum_{i=1}^N e^{i\mathbf{q}\cdot\mathbf{r}_i} - \frac{N}{V} \delta_{\mathbf{q},0}, \quad (4)$$

with N is the number of particles, V the volume, and \mathbf{r}_i is the position of particle i . The structure factor measures the spatial correlations of particle positions, but it does not show any diverging peak in contrast to what happens, for example, at the liquid-gas tri-critical point where there it has a divergence at small \mathbf{q} . More complicated static correlation functions have been studied [10], especially in numerical work, but until now there are no strong indications of a diverging, or at least substantially growing, static lengthscale [11]. A snapshot of a supercooled liquid configuration in fact just looks like a glass configuration, despite their widely different dynamic properties. What happens then at the glass transition? Is it a transition or simply a dynamic crossover?

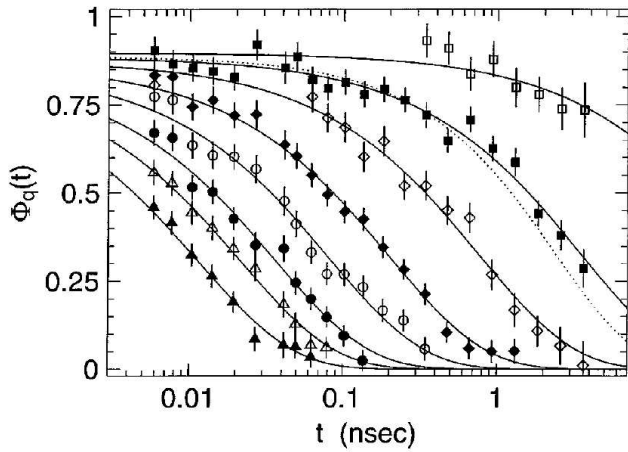


FIG. 2: Temperature evolution of the intermediate scattering function normalized by its value at time equal to zero for supercooled glycerol [12]. Temperatures decrease from 413 K to 270 K from left to right. The solid lines are fit with a stretched exponential with exponent $\beta = 0.7$. The dotted line represents another fit with $\beta = 0.82$.

A more refined understanding can be gained studying dynamic correlations or response functions.

A dynamic observable studied in light and neutron scattering experiments is the intermediate scattering function,

$$F(\mathbf{q}, t) = \left\langle \frac{1}{N} \delta\rho_{\mathbf{q}}(t) \delta\rho_{-\mathbf{q}}(0) \right\rangle. \quad (5)$$

Different $F(\mathbf{q}, t)$ measured by neutron scattering in supercooled glycerol [12] are shown for different temperatures in Fig. 2. These curves show a first, rather fast, relaxation to a plateau followed by a second, much slower, relaxation. The plateau is due to the fraction of density fluctuations that are frozen on intermediate timescales, but eventually relax during the second relaxation. The latter is called ‘alpha-relaxation’, and corresponds to the structural relaxation of the liquid. This plateau is akin to the Edwards-Anderson order parameter, q_{EA} , defined for spin glasses which measures the fraction of frozen spin fluctuations [13]. Note that q_{EA} continuously increases from zero below the spin glass transition. Instead, for structural glasses, a finite plateau appears above any transition.

The intermediate scattering function can be probed only on a relatively small regime of temperatures. In order to track the dynamic slowing down from microscopic to macroscopic timescales, other correlators have been studied. A popular one is obtained from the dielectric susceptibility, which is related by the fluctuation-dissipation theorem to the time correlation of polarization fluctuations. It is generally admitted that different dynamic probes reveal similar temperature dependences for the relaxation time. The temperature evolution of the imaginary part of the dielectric susceptibility, $\epsilon''(\omega)$,

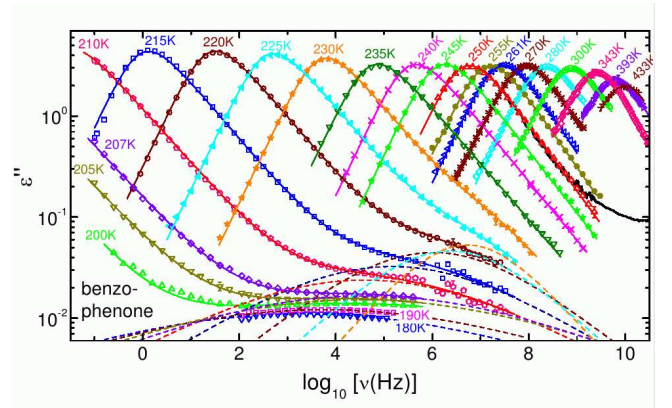


FIG. 3: Temperature evolution of the dielectric susceptibility of the glass-former benzophenone measured over more than 10 decades of relaxation times [14]. Dynamics slows down dramatically as temperature is decreased and relaxation spectra become very broad at low temperature.

is shown in Fig. 3 which covers a very wide temperature window [14]. At high temperature, a good representation of the data is given by a Debye law, $\epsilon(\omega) = \epsilon(\infty) + \Delta\epsilon/(1 + i\omega\tau_\alpha)$, which corresponds to an exponential relaxation in the time domain. When temperature is decreased, however, the relaxation spectra become very broad and strongly non-Debye. One particularly well-known feature of the spectra is that they are well fitted, in the time domain, for times corresponding to the alpha-relaxation with a stretched exponential, $\exp(-(t/\tau_\alpha)^\beta)$. In the Fourier domain, forms such as the Havriliak-Negami law are used, $\epsilon(\omega) = \epsilon(\infty) + \Delta\epsilon/(1 + (i\omega\tau_\alpha)^\alpha)^\gamma$, which generalizes the Debye law. The exponents β , α and γ depend in general on temperature and on the particular dynamic probe chosen, but they capture the fact that relaxation is increasingly non-exponential when T decreases towards T_g . A connection was empirically established between fragility and degree of non-exponentiality, more fragile liquids being characterized by broader relaxation spectra [2].

To sum up, there are many remarkable phenomena that take place when a supercooled liquid approaches the glass transition. Striking ones have been presented, but many others have been left out for lack of space [1, 2, 10, 13]. We have discussed physical behaviours, relationships or empirical correlations observed in a broad class of materials. This is quite remarkable and suggests that there is some physics (and not only chemistry) to the problem of the glass transition, which we see as a collective (critical?) phenomenon relatively independent of microscopic details. This justifies our statistical mechanics perspective on this problem.

IV. TAXONOMY OF ‘GLASSES’ IN SCIENCE

We now introduce some other systems whose phenomenological behaviour is close or, at least, related, to the one of glass-forming liquids, showing that glassiness is truly ubiquitous. It does not only appear in many different physical situations but also in more abstract contexts, such as computer science.

A. The jamming transition of colloids and grains

Colloidal suspensions consist of big particles suspended in a solvent [15]. The typical radii of the particles are in the range $R = 1 - 500$ nm. The solvent, which is at equilibrium at temperature T , makes the short-time dynamics of the particles Brownian. The microscopic timescale for this diffusion is given by $\tau = R^2/D$ where D is the short-time self-diffusion coefficient. Typical values are of the order of $\tau \sim 1$ ms, and thus are much larger than the ones for molecular liquids (in the picosecond regime). The interaction potential between particles depends on the systems, and this large tunability makes colloids very attractive objects for technical applications. A particularly relevant case, on which we will focus in the following, is a purely hard sphere potential, which is zero when particles do not overlap and infinite otherwise. In this case the temperature becomes irrelevant, apart from a trivial rescaling of the microscopic timescale. Colloidal hard spheres systems have been intensively studied [15] in experiments, simulations and theory varying their density ρ , or their volume fraction $\phi = \frac{4}{3}\pi R^3\rho$. Hard spheres display a fluid phase from 0 to intermediate volume fractions, a freezing-crystallisation transition at $\phi \simeq 0.494$, and a melting transition at $\phi \simeq 0.545$. Above this latter value the system can be compressed until the close packing point $\phi \simeq 0.74$, which corresponds to the FCC crystal. Interestingly for our purposes, a small amount of polydispersity (particles with slightly different sizes) suppresses crystallization. In this case, the system can be more easily ‘supercompressed’ above the freezing transition without nucleating the crystal, at least on experimental timescales. In this regime the relaxation timescale increases very fast [16]. At a packing fraction $\phi_g \simeq 0.58$ it becomes so large compared to typical experimental timescales that the system does not relax anymore: it is jammed. This ‘jamming transition’ is obviously reminiscent of the glass transition of molecular systems. In particular, the location ϕ_g of the colloidal glass transition is as ill-defined as the glass temperature T_g .

Actually, the phenomena that take place increasing the volume fraction are analogous to the ones seen in molecular supercooled liquid: the relaxation timescales increase very fast and can be fitted [17] by a VFT law in density as in Eq. (1), dynamical correlation functions display a broad spectrum of timescales and develop a plateau, no static growing correlation length has been found, etc. Also the phenomenon of dynamic hetero-

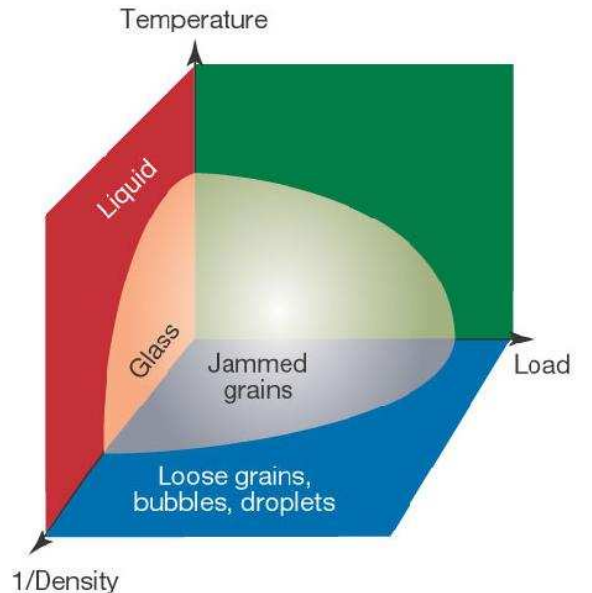


FIG. 4: The ‘great unification’ phase diagram of jamming and glass transitions [25]. Glassy phases occur at low temperature, low external drive, or high density in different systems.

geneity that will be addressed in Sec. VI is present in both cases [18–20]. However, it is important to underline a major difference: because the microscopic timescale for colloids is so large, experiments can only track the first 5 decades of slowing down. A major consequence is that the comparison between the glass and colloidal transitions must be performed by focusing in both cases on the first 5 decades of the slowing down, which corresponds to relatively high temperatures in molecular liquids. Understanding how much and to what extent the glassiness of colloidal suspensions is related to the one of molecular liquids remains an active domain of research.

Another class of systems that have recently been studied from the point of view of their glassiness is driven granular media. Grains are macroscopic objects and, as a consequence, do not have any thermal motion. A granular material is therefore frozen in a given configuration if no energy is injected into the system [21]. However, it can be forced in a steady state by an external drive, such as shearing or tapping. The dynamics in this steady state shows remarkable similarities (and differences) with simple fluids. The physics of granular materials is a very wide subject [21]. In the following we only address briefly what happens to a polydisperse granular fluid at very high packing fractions, close to its random close packed state. As for colloids, the timescales for relaxation or diffusion increase very fast when density is increased, without any noticeable change in structural properties. Again, it is now established [22–24] that many phenomenological properties of the glass and jamming transitions also occur in granular assemblies. As for colloids, going beyond the mere analogy and under-

standing how much these different physical systems are related is a very active domain of research.

This very question has been asked in a visual manner by Liu and Nagel [25] who rephrased it in a single picture, reproduced in Fig. 4. By building a common phase diagram for glasses, colloids and grains, they ask whether the glass and jamming transitions of molecular liquids, colloids and granular media are different facets of the same phase. In this unifying ‘phase diagram’, the ‘phase’ close to the origin is glassy and can be reached either by lowering the temperature as in molecular liquids, or increasing the packing fraction or decreasing the external drive in colloids and granular media. It remains to provide precise answers to this elegantly formulated, rather broad, set of questions.

B. Other ‘glasses’ in physics and beyond

There are many other physical contexts in which glassiness plays an important role [4]. A most famous example is the field of spin glasses. Real spin glasses are magnetic impurities interacting by quenched random couplings. At low temperatures, their dynamics become extremely slow and they freeze in amorphous spin configuration dubbed a ‘spin glass’ by P.W. Anderson. There are many other physical systems, often characterized by quenched disorder, that show glassy behaviour, like Coulomb glasses, Bose glasses, etc. In many cases, however, one does expect quite a different physics from structural glasses: the similarity between these systems is therefore only qualitative.

Finally, and quite remarkably, glassiness emerges even in other branches of science [5]. In particular, it has been discovered recently that concepts and techniques developed for glassy systems turn out to apply and be very useful tools in the field of computer science. Problems like combinatorial optimization display phenomena completely analogous to phase transitions, actually, to glassy phase transitions. *A posteriori*, this is quite natural, because a typical optimization problem consists in finding a solution in a presence of a large number of constraints. This can be defined, for instance, as a set of N Boolean variables that satisfies M constraints. For N and M very large at fixed $\alpha = M/N$, this problem very much resembles finding a ground state in a statistical mechanics problem with quenched disorder. Indeed one can define an energy function (a Hamiltonian) as the number of unsatisfied constraints, that has to be minimized, as in a $T = 0$ statmech problem. The connection with glassy systems origins from the fact that in both cases the energy landscape is extremely complicated, full of minima and saddles. The fraction of constraints per degree of freedom, α , plays a role similar to the density in a hard sphere system. A detailed presentation of the relationship between optimization problems and glassy systems is clearly out of the scope of the present review. We simply illustrate it pointing out that a central problem

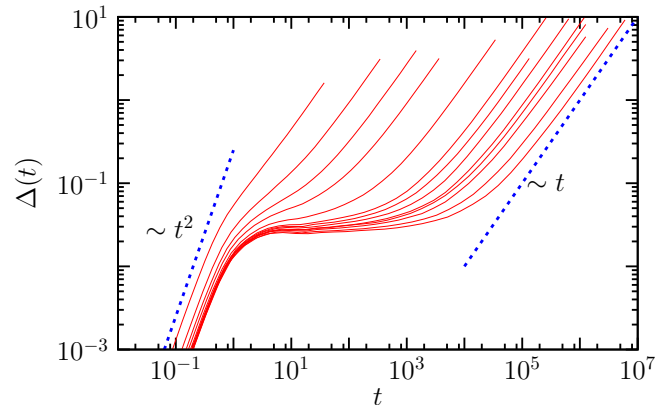


FIG. 5: Mean-squared displacements of individual particles in a simple model of a glass-forming liquid composed of Lennard-Jones particles observed on a wide time window. When temperature decreases (from left to right), the particle displacements become increasingly slow with several distinct time regimes corresponding, in this order, to ballistic, localized, and diffusive regimes.

in optimization, random k -satisfiability, has been shown to undergo a glass transition when α increases that is analogous to the one of structural glasses [26].

V. NUMERICAL SIMULATIONS

Studying the glass transition of molecular liquids at a microscopic level is in principle straightforward since one must answer a very simple question: how do particles move in a liquid close to T_g ? It is of course a daunting task to attempt answering this question experimentally because one should then resolve the dynamics of single molecules to be able to follow the trajectories of objects that are a few Angstroms large on timescales of tens or hundreds of seconds, which sounds like eternity when compared to typical molecular dynamics usually lying in the picosecond regime. In recent years, such direct experimental investigations have been started using time and space resolved techniques such as atomic force microscopy [27] or single molecule spectroscopy [28], but this remains a very difficult task.

In numerical simulations, by contrast, the trajectory of each particle in the system can, by construction, be followed at all times. This allows one to quantify easily single particle dynamics, as proved in Fig. 5 where the averaged mean-squared displacement $\Delta(t)$ measured in a simple Lennard-Jones glass-former is shown. It is defined by

$$\Delta(t) = \left\langle \frac{1}{N} \sum_{i=1}^N |\mathbf{r}_i(t) - \mathbf{r}_i(0)|^2 \right\rangle, \quad (6)$$

where $\mathbf{r}_i(t)$ represents the position of particle i at time t in a system composed of N particles; the brackets indicate an ensemble average. The particle displacements

considerably slow down when T is decreased and the self-diffusion constant decreases by orders of magnitude, mirroring the behaviour of the viscosity shown in Fig. 1 for real systems. Moreover, a rich dynamics is observed, with a plateau regime at intermediate timescales, corresponding to an extended time window during which particles vibrate around their initial positions, exactly as in a crystalline solid. The difference with a crystal is of course that this localization is only transient, and all particles eventually escape and diffuse at long times with a diffusion constant D_s , so that $\Delta(t) \sim 6D_s t$ when $t \rightarrow \infty$.

In recent years, computer experiments have played an increasingly important role in glass transition studies. It could almost be said that particle trajectories in numerical work have been studied under so many different angles that probably very little remains to be learnt from such studies in the regime that is presently accessible using present day computers. Unfortunately, this does not imply complete knowledge of the physics of supercooled liquids. As shown in Fig. 5, it is presently possible to follow the dynamics of a simple glass-forming liquid over more than eight decades of time, and over a temperature window in which average relaxation timescales increase by more than five decades. This might sound impressive, but a quick look at Fig. 1 shows, however, that at the lowest temperatures studied in the computer, the relaxation timescales are still orders of magnitude faster than in experiments performed close to the glass transition temperature. They can be directly compared to experiments performed in this high temperature regime, but this also implies that simulations focus on a relaxation regime that is about eight to ten decades of times faster than in experiments performed close to T_g . Whether numerical works are useful to understand the glass transition itself at all is therefore an open, widely debated, question. We believe that it is now possible to numerically access temperatures which are low enough that many features associated to the glass transition physics can be observed: strong decoupling phenomena, clear deviations from fits to the mode-coupling theory (which are experimentally known to hold only at high temperatures), and crossovers towards truly activated dynamics.

Classical computer simulations of supercooled liquids usually proceed by solving a cleverly discretized version of Newton's equations for a given potential interaction between particles [29]. If quantitative agreement with experimental data on an existing specific material is sought, the interaction must be carefully chosen in order to reproduce reality, for instance by combining classical to *ab-initio* simulations. From a more fundamental perspective one rather seeks the simplest model that is still able to reproduce qualitatively the phenomenology of real glass-formers, while being considerably simpler to study. The implicit, but quite strong, hypothesis is that molecular details are not needed to explain the behaviour of supercooled liquids, so that the glass transition is indeed a topic for statistical mechanics, not for chemistry. A considerable amount of work has therefore

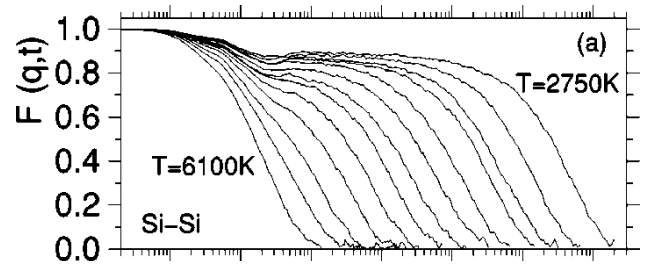


FIG. 6: Intermediate scattering function at wavevector 1.7 \AA^{-1} for the Si particles at $T = 2750 \text{ K}$ obtained from molecular dynamics simulations of a model for silica [30].

been dedicated to studying models such as hard spheres, soft spheres, or Lennard-Jones particles. More realistic materials are also studied focusing for instance on the physics of network forming materials, multi-component ones, anisotropic particles, or molecules with internal degrees of freedom. Connections to experimental work can be made by computing quantities that are experimentally accessible such as the intermediate scattering function, static structure factors, $S(\mathbf{q})$, or thermodynamic quantities such specific heat or configurational entropy, which are directly obtained from particle trajectories and can be measured in experiments as well. As an example we show in Fig. 6 the intermediate scattering function $F(\mathbf{q}, t)$ obtained from a molecular dynamics simulation of a classical model for SiO_2 as a function of time for different temperatures [30].

An important role is played by simulations also because a large variety of dynamic and static quantities can be simultaneously measured in a single model system. As we shall discuss below, there exist scores of different theoretical approaches to describe the physics of glass-formers, and they sometimes have their own set of predictions that can be readily tested by numerical work. Indeed, quite a large amount of numerical papers have been dedicated to testing in detail the predictions formulated by the mode-coupling theory of the glass transition, as reviewed recently in Ref. [31]. Here, computer simulations are particularly well-suited as the theory specifically addresses the relatively high temperature window that is studied in computer simulations.

While Newtonian dynamics is mainly used in numerical work on supercooled liquids, a most appropriate choice for these materials, it can be interesting to consider alternative dynamics that are not deterministic, or which do not conserve the energy. In colloidal glasses and physical gels, for instance, particles undergo Brownian motion arising from collisions with molecules in the solvent, and a stochastic dynamics is more appropriate. Theoretical considerations might also suggest the study of different sorts of dynamics for a given interaction between particles, for instance, to assess the role of conservation laws and structural information. Of course, if a given stochastic dynamics satisfies detailed balance with respect to the Boltzmann distribution, all structural

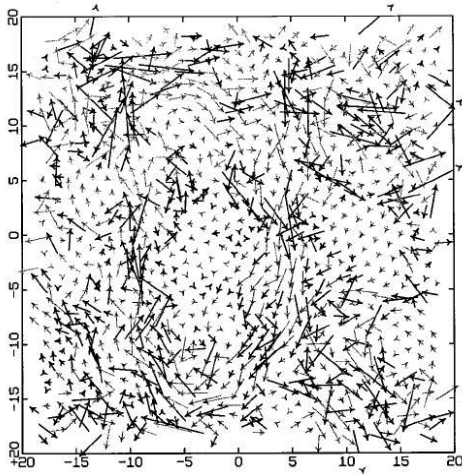


FIG. 7: Spatial map of single particle displacements in the simulation of a binary mixture of soft spheres in two dimensions [38]. Arrows show the displacement of each particle in a trajectory of length about 10 times the structural relaxation time. The map reveals the existence of particles with different mobilities during relaxation, but also the existence of spatial correlations between these dynamic fluctuations.

quantities remain unchanged, but the resulting dynamical behaviour might be very different. Several papers [32–34] have studied in detail the influence of the chosen microscopic dynamics on the dynamical behaviour in glassformers using either stochastic dynamics (where a friction term and a random noise are added to Newton’s equations, the amplitude of both terms being related by a fluctuation-dissipation theorem), Brownian dynamics (in which there are no momenta, and positions evolve with Langevin dynamics), or Monte-Carlo dynamics (where the potential energy between two configurations is used to accept or reject a trial move). Quite surprisingly, the equivalence between these three types of stochastic dynamics and the originally studied Newtonian dynamics was established at the level of the averaged dynamical behaviour [32–34], except at very short times where obvious differences are indeed expected. This strongly suggests that an explanation for the appearance of slow dynamics in these materials originates from their amorphous structure. However, important differences were found when dynamic fluctuations were considered [34–36], even in the long-time regime comprising the structural relaxation.

Another crucial advantage of molecular simulations is illustrated in Fig. 7. This figure shows a spatial map of single particle displacements recorded during the simulation of a binary soft sphere system in two dimensions [38]. This type of measurement, out of reach of most experimental techniques that study the liquid state, reveals that dynamics might be very different from one particle to another. More importantly, Fig. 7 also unambiguously reveals the existence of spatial correlations between these dynamic fluctuations. The presence of non-trivial spatio-temporal fluctuations in supercooled liquids is now called

‘dynamic heterogeneity’ [39]. This is the phenomenon we discuss in more detail in the next section.

VI. DYNAMIC HETEROGENEITY

A. Existence of spatio-temporal dynamic fluctuations

A new facet of the relaxational behaviour of supercooled liquids has emerged in the last decade thanks to a considerable experimental and theoretical effort. It is called ‘dynamic heterogeneity’ (DH), and plays now a central role in modern descriptions of glassy liquids [39]. As anticipated in the previous section, the phenomenon of dynamic heterogeneity is related to the spatio-temporal fluctuations of the dynamics. Initial motivations stemmed from the search for an explanation of the non-exponentiality of relaxation processes in supercooled liquids, related to the existence of a broad relaxation spectrum. Two natural, but fundamentally different, explanations can be put forward. (1) The relaxation is locally exponential, but the typical relaxation timescale varies spatially. Hence, global correlation or response functions become non-exponential upon spatial averaging over this spatial distribution of relaxation times. (2) The relaxation is complicated and inherently non-exponential, even locally. Experimental and theoretical works [39] suggest that both mechanisms are likely at play, but definitely conclude that relaxation is spatially heterogeneous, with regions that are faster and slower than the average. Since supercooled liquids are ergodic materials, a slow region will eventually become fast, and vice-versa. A physical characterization of DH entails the determination of the typical lifetime of the heterogeneities, as well as their typical lengthscale.

A clear and more direct confirmation of the heterogeneous character of the dynamics also stems from simulation studies. For example, whereas the simulated average mean-squared displacements are smooth functions of time, time signals for individual particles clearly exhibit specific features that are not observed unless dynamics is resolved both in space and time. These features are displayed in Fig. 8. What do we see? We mainly observe that particle trajectories are not smooth but rather composed of a succession of long periods of time where particles simply vibrate around well-defined locations, separated by rapid ‘jumps’. Vibrations were previously inferred from the plateau observed at intermediate times in the mean-squared displacements of Fig. 5, but the existence of jumps that are clearly statistically widely distributed in time cannot be guessed from averaged quantities only. The fluctuations in Fig. 8 suggest, and direct measurements confirm, the importance played by fluctuations around the averaged dynamical behaviour.

A simple type of such fluctuations has been studied in much detail. When looking at Fig. 8, it is indeed natural to ask, for any given time, what is the distribution of

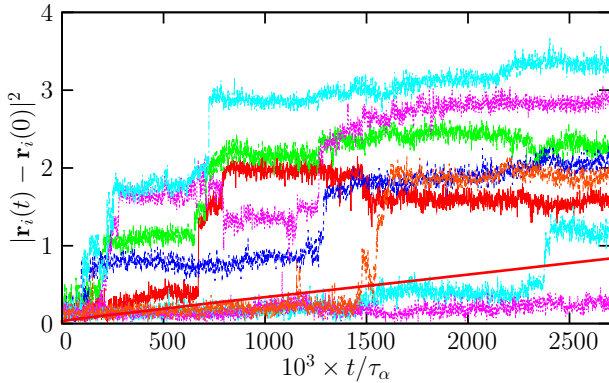


FIG. 8: Time resolved squared displacements of individual particles in a simple model of a glass-forming liquid composed of Lennard-Jones particles. The average is shown as a smooth full line. Trajectories are composed of long periods of time during which particles vibrate around well-defined positions, separated by rapid jumps that are widely distributed in time underlying the importance of dynamic fluctuations.

particle displacements. This is quantified by the self-part of the van-Hove function defined as

$$G_s(\mathbf{r}, t) = \left\langle \frac{1}{N} \sum_{i=1}^N \delta(\mathbf{r} - [\mathbf{r}_i(t) - \mathbf{r}_i(0)]) \right\rangle. \quad (7)$$

For an isotropic Gaussian diffusive process, one gets $G_s(\mathbf{r}, t) = \exp(-|\mathbf{r}|^2/(4D_s t))/(4\pi D_s t)^{3/2}$. Simulations reveal instead strong deviations from Gaussian behaviour on the timescales relevant for structural relaxation [40]. In particular they reveal ‘fat’ tails in the distributions that are much wider than expected from the Gaussian approximation. These tails are in fact well described by an exponential, rather than Gaussian, decay in a wide time window comprising the structural relaxation, such that $G_s(\mathbf{r}, t) \sim \exp(-|\mathbf{r}|/\lambda(t))$ [41]. Thus, they reflect the existence of a population of particles that move distinctively further than the rest and appear therefore to be much more mobile. This observation implies that relaxation in a viscous liquid differs qualitatively from that of a normal liquid where diffusion is close to Gaussian, and that a non-trivial statistics of single particle displacements exists.

A long series of questions immediately follows this seemingly simple observation. Answering them has been the main occupation of many workers in this field over the last decade. What are the particles in the tails effectively doing? Why are they faster than the rest? Are they located randomly in space or do they cluster? What is the geometry, time and temperature evolution of the clusters? Are these spatial fluctuations correlated to geometric or thermodynamic properties of the liquids? Do similar correlations occur in all glassy materials? Can one predict these fluctuations theoretically? Can one understand glassy phenomenology using fluctuation-based arguments? Can these fluctuations be detected experimentally?

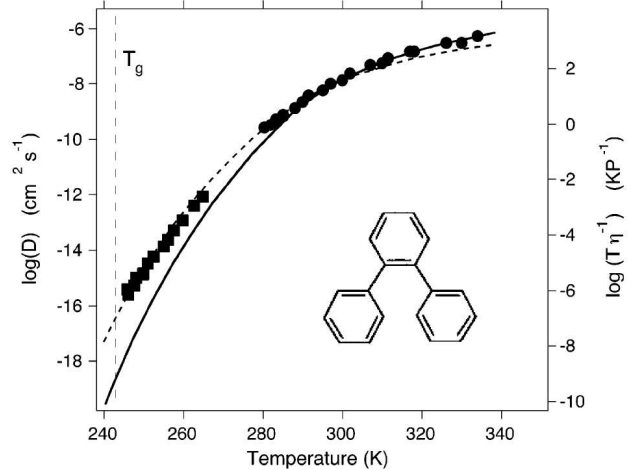


FIG. 9: Decoupling between viscosity (full line) and self-diffusion coefficient (symbols) in supercooled ortho-terphenyl [43]. The dashed line shows a fit with a ‘fractional’ Stokes-Einstein relation, $D_s \sim (T/\eta)^\zeta$ with $\zeta \sim 0.82$.

Another influential phenomenon that was related early on to the existence of DH is the decoupling of self-diffusion (D_s) and viscosity (η). In the high temperature liquid self-diffusion and viscosity are related by the Stokes-Einstein relation [42], $D_s \eta / T = \text{const.}$ For a large particle moving in a fluid the constant is equal to $1/(6\pi R)$ where R is the particle radius. Physically, the Stokes-Einstein relation means that two different measures of the relaxation time R^2/D_s and $\eta R^3/T$ lead to the same timescale up to a constant factor. In supercooled liquids this phenomenological law breaks down, as shown in Fig. 9 for ortho-terphenyl [43]. It is commonly found that D_s^{-1} does not increase as fast as η so that, at T_g , the product $D_s \eta$ has increased by 2-3 orders of magnitude as compared to its Stokes-Einstein value. This phenomenon, although less spectacular than the overall change of viscosity, is a significant indication that different ways to measure relaxation times lead to different answers and, thus, is a strong hint of the existence of a distribution of relaxation timescales.

Indeed, a natural explanation of this effect is that different observables probe in different ways the underlying distribution of relaxation times [39]. For example, the self-diffusion coefficient of tracer particles is dominated by the more mobile particles whereas the viscosity or other measures of structural relaxation probe the timescale needed for every particle to move. An unrealistic but instructive example is a model where there is a small, non-percolative subset of particles that are blocked forever, coexisting with a majority of mobile particles. In this case, the structure never relaxes but the self-diffusion coefficient is non-zero because of the mobile particles. Of course, in reality all particles move, eventually, but this shows how different observables are likely to probe different moments of the distribution of

5 – 10 molecule diameters [39].

B. Multi-point correlation functions

More recently, substantial progress in characterizing spatio-temporal dynamical fluctuations was obtained from theoretical [35–37, 47, 48] and numerical results [38, 49–52]. In particular, it is now understood that dynamical fluctuations can be measured and characterized through the use of four-point correlation functions. These multi-point functions can be seen as a generalization of the spin glass susceptibility measuring the extent of amorphous long-range order in spin glasses. In this subsection, we introduce these correlation functions and summarize the main results obtained using them.

Standard experimental probes of the averaged dynamics of liquids give access to the time-dependent auto-correlation function of the spontaneous fluctuations of some observable $O(t)$, $F(t) = \langle \delta O(0) \delta O(t) \rangle$, where $\delta O(t) = O(t) - \langle O \rangle$ represents the instantaneous value of the deviation of $O(t)$ from its ensemble average $\langle O \rangle$ at time t . One can think of $F(t)$ as being the average of a two-point quantity, $C(0, t) = \delta O(0) \delta O(t)$, characterizing the dynamics. A standard example corresponds to O being equal to the Fourier transform of the density field. In this case $F(t)$ is the dynamical structure factor as in Eq. (5). More generally, the correlation functions $F(t)$ measure the global relaxation in the system. Intuitively, in a system with important dynamic correlations, the fluctuations of $C(0, t)$ will be stronger. Quantitative information on the amplitude of those fluctuations is provided by the variance

$$\chi_4(t) = N \langle \delta C(0, t)^2 \rangle, \quad (8)$$

where $\delta C(0, t) = C(0, t) - F(t)$, and N is the total number of particles in the system. The associated spatial correlations show up more clearly when considering a ‘local’ probe of the dynamics, like for instance an orientational correlation function measured by dielectric or light scattering experiments, which can be expressed as

$$C(0, t) = \frac{1}{V} \int d^3r c(\mathbf{r}; 0, t), \quad (9)$$

where V is the volume of the sample and $c(\mathbf{r}; 0, t)$ characterizes the dynamics between times 0 and t around point \mathbf{r} . For example, in the above mentioned case of orientational correlations, $c(\mathbf{r}; 0, t) \propto \frac{V}{N} \sum_{i,j=1}^N \delta(\mathbf{r} - \mathbf{r}_i) Y(\Omega_i(0)) Y(\Omega_j(t))$, where Ω_i denotes the angles describing the orientation of molecule i , $\mathbf{r}_i(0)$ is the position of that molecule at time 0, and $Y(\Omega)$ is some appropriate rotation matrix element. Here, the ‘locality’ of the probe comes from the fact that it is dominated by the self-term involving the same molecule at times 0 and t , or by the contribution coming from neighboring molecules. The dynamic susceptibility $\chi_4(t)$ can thus be rewritten as

$$\chi_4(t) = \rho \int d^3r G_4(\mathbf{r}; 0, t), \quad (10)$$

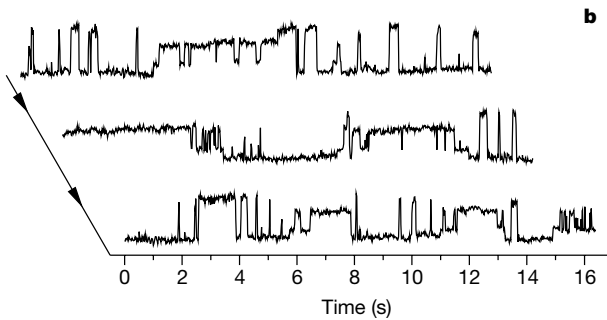


FIG. 10: Time series of polarization in the AFM experiment performed by Vidal Russell and Israeloff [27] on PVAc at $T = 300$ K. The signal intermittently switches between periods with fast or slow dynamics, suggesting that extended regions of space indeed transiently behave as fast and slow regions.

timescales, as explicitly shown within several theoretical frameworks [44, 45].

The phenomena described above, although certainly an indication of spatio-temporal fluctuations, do not allow one to study how these fluctuations are correlated in space. This is, however, a fundamental issue both from the experimental and theoretical points of view. How large are the regions that are faster or slower than the average? How does their size depend on temperature? Are these regions compact or fractal? These important questions were first addressed in pioneering works using four-dimensional NMR [46], or by directly probing fluctuations at the nanoscopic scale using microscopy techniques. In particular, Vidal Russell and Israeloff using Atomic Force Microscopy techniques [27] measured the polarization fluctuations in a volume of size of few tens of nanometers in a supercooled polymeric liquid (PVAc) close to T_g . In this spatially resolved measurement, the hope is to probe a small enough number of dynamically correlated regions, and detect their dynamics. Indeed, the signal shown in Fig. 10 shows a dynamics which is very intermittent in time, the dynamics switching between moments with intense activity, and moments with no dynamics at all, suggesting that extended regions of space indeed transiently behave as fast and slow regions. A much smoother signal would have been measured if these such dynamically correlated ‘domains’ were not present. Spatially resolved and NMR experiments are quite difficult. They give undisputed information about the typical lifetime of the DH, but their determination of a dynamic correlation lengthscale is rather indirect and/or performed on a small number of liquids in a small temperature window. Nevertheless, the outcome is that a non-trivial dynamic correlation length emerges at the glass transition, where it reaches a value of the order of

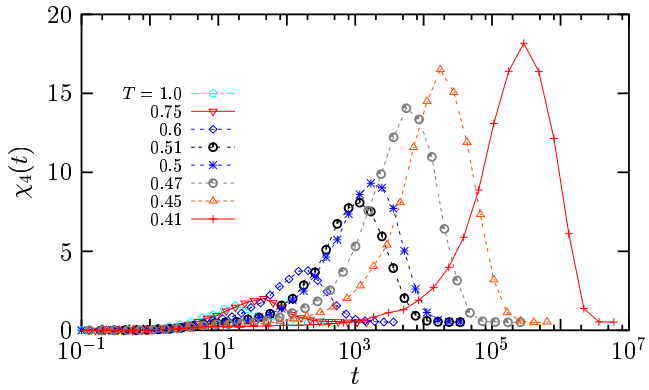


FIG. 11: Time dependence of $\chi_4(t)$ quantifying the spontaneous fluctuations of the intermediate scattering function in a Lennard-Jones supercooled liquid. For each temperature, $\chi_4(t)$ has a maximum, which shifts to larger times and has a larger value when T is decreased, revealing the increasing lengthscale of dynamic heterogeneity in supercooled liquids approaching the glass transition.

where

$$G_4(\mathbf{r}; 0, t) = \langle \delta c(\mathbf{0}; 0, t) \delta c(\mathbf{r}; 0, t) \rangle, \quad (11)$$

and translational invariance has been taken into account ($\rho = N/V$ denotes the mean density). The above equations show that $\chi_4(t)$ measures the extent of spatial correlation between dynamical events between times 0 and t at different points of the system, *i.e.*, the spatial extent of dynamically heterogeneous regions over a time span t .

The function $\chi_4(t)$ has been measured by molecular dynamics, Brownian and Monte Carlo simulations in different liquids [50–54]. An example is shown in Fig. 11 for a Lennard-Jones liquid. The qualitative behaviour is similar in all cases [35, 47, 48]: as a function of time $\chi_4(t)$ first increases, it has a peak on a timescale that tracks the structural relaxation timescale and then it decreases [178]. The peak value measures thus the volume on which the structural relaxation processes are correlated. It is found to increase when the temperature decreases and the dynamics slows down. By measuring directly $G_4(\mathbf{r}; 0, t)$ it has also been checked that the increase of the peak of $\chi_4(t)$ corresponds, as expected, to a growing dynamic lengthscale ξ [35, 51, 52], although these measurements are much harder in computer simulations, because very large systems need to be simulated to determine ξ unambiguously. Note that if the dynamically correlated regions were compact, the peak of χ_4 would be proportional to ξ^3 in three dimensions, directly relating χ_4 measurements to that of the relevant lengthscale of DH.

These results are also relevant because many theories of the glass transition assume or predict, in a way or another, that the dynamics slows down because there are increasingly large regions on which particles have to relax in a correlated or cooperative way. However, this lengthscale remained elusive for a long time. Measures

of the spatial extent of dynamic heterogeneity, in particular $\chi_4(t)$ and $G_4(\mathbf{r}; 0, t)$, seem to provide the long-sought evidence of this phenomenon. This in turn suggests that the glass transition is indeed a critical phenomenon characterized by growing timescales and lengthscales. A clear and conclusive understanding of the relationship between the lengthscale obtained from $G_4(\mathbf{r}; 0, t)$ and the relaxation timescale is still the focus of an intense research activity.

One major issue is that obtaining information on the behaviour of $\chi_4(t)$ and $G_4(\mathbf{r}; 0, t)$ from experiments is difficult. Such measurements are necessary because numerical simulations can only be performed rather far from T_g , see Sec. V. Up to now, direct experimental measurements of $\chi_4(t)$ have been restricted to colloidal [56] and granular materials [24, 55] close to the jamming transition, because dynamics is more easily spatially resolved in those cases. Unfortunately, similar measurements are currently not available in molecular liquids.

Recently, an approach based on fluctuation-dissipation relations and rigorous inequalities has been developed in order to overcome this difficulty [35, 36, 57]. The main idea is to obtain a rigorous lower bound on $\chi_4(t)$ using the Cauchy-Schwarz inequality $\langle \delta H(0) \delta C(0, t) \rangle^2 \leq \langle \delta H(0)^2 \rangle \langle \delta C(0, t)^2 \rangle$, where $H(t)$ denotes the enthalpy at time t . By using fluctuation-dissipation relations the previous inequality can be rewritten as [57]

$$\chi_4(t) \geq \frac{k_B T^2}{c_P} [\chi_T(t)]^2, \quad (12)$$

where the multi-point response function $\chi_T(t)$ is defined by

$$\chi_T(t) = \left. \frac{\partial F(t)}{\partial T} \right|_{N,P} = \frac{N}{k_B T^2} \langle \delta H(0) \delta C(0, t) \rangle. \quad (13)$$

In this way, the experimentally accessible response $\chi_T(t)$ which quantifies the sensitivity of average correlation functions $F(t)$ to an infinitesimal temperature change, can be used in Eq. (12) to yield a lower bound on $\chi_4(t)$. Moreover, detailed numerical simulations and theoretical arguments [35, 36] strongly suggest that the right hand side of (12) actually provides a good estimation of $\chi_4(t)$, not just a lower bound.

Using this method, Dalle-Ferrier *al.* [58] have been able to obtain the evolution of the peak value of χ_4 for many different glass-formers in the entire supercooled regime. In Fig. 12 we show some of these results as a function of the relaxation timescale. The value on the y -axis, the peak of χ_4 , is a proxy for the number of molecules, $N_{\text{corr},4}$ that have to evolve in a correlated way in order to relax the structure of the liquid. Note that χ_4 is expected to be equal to $N_{\text{corr},4}$, up to a proportionality constant which is not known from experiments, probably explaining why the high temperature values of $N_{\text{corr},4}$ are smaller than one. Figure 12 also indicates that $N_{\text{corr},4}$ grows faster when τ_α is not very large, close to the onset of slow dynamics, and a power law relationship between $N_{\text{corr},4}$ and

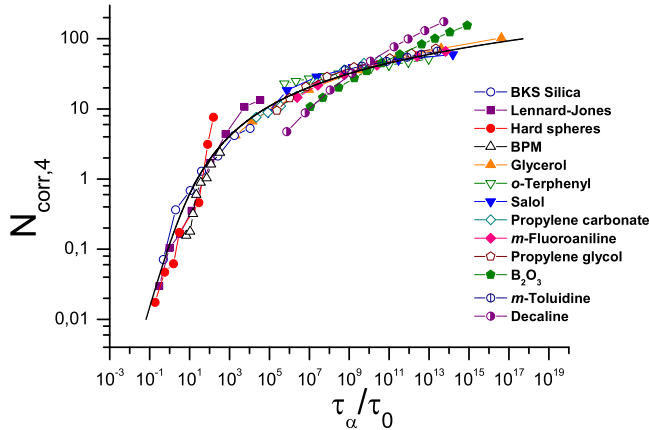


FIG. 12: Universal dynamic scaling relation between number of dynamically correlated particles, $N_{\text{corr},4}$, and relaxation timescale, τ_α , for a number of glass-formers [58], determined using Eq. (12).

τ_α is good in this regime ($\tau_\alpha/\tau_0 < 10^4$). The growth of $N_{\text{corr},4}$ becomes much slower closer to T_g . A change of 6 decades in time corresponds to a mere increase of a factor about 4 of $N_{\text{corr},4}$, suggesting logarithmic rather than power law growth of dynamic correlations. This is in agreement with several theories of the glass transition which are based on activated dynamic scaling [59–61].

Understanding quantitatively this relation between timescales and lengthscales is one of the main recent topics addressed in theories of the glass transition, see the next section. Furthermore, numerical works are also devoted to characterizing better the geometry of the dynamically heterogeneous regions [62, 63].

VII. SOME THEORY AND MODELS

We now present some theoretical approaches to the glass transition. It is impossible to cover all of them in a brief review, simply because there are way too many of them, perhaps the clearest indication that the glass transition remains an open problem. We choose to present approaches that are keystones and have a solid statistical mechanics basis. Loosely speaking, they have an Hamiltonian, can be simulated numerically, or studied analytically with statistical tools. Of course, the choice of Hamiltonians is crucial and contains very important assumptions about the nature of the glass transition. All these approaches have given rise to unexpected results. One finds more in them than what was supposed at the beginning, which leads to new, testable predictions. Furthermore, with models that are precise enough, one can test (and hopefully falsify!) these approaches by working out all their predictions in great detail, and comparing the outcome to experimental data. This is not possi-

ble with ‘physical pictures’, or simpler approaches of the problem which we have therefore avoided.

Before going into the models, we would like to state the few important questions that face theoreticians.

- Why do the relaxation time and the viscosity increase when T_g is approached? Why is this growth super-Arrhenius?
- Can one understand and describe quantitatively the average dynamical behaviour of supercooled liquids, in particular broad relaxation spectra, non-exponential behaviour, and their evolution with fragility?
- What is the underlying reason of the apparent relation between kinetics and thermodynamics (like $T_0 \simeq T_K$)?
- Can one understand and describe quantitatively the spatio-temporal fluctuations of the dynamics? How and why are these fluctuations related to the dynamic slowing down?
- Is the glass transition a collective phenomenon? If yes, of which kind? Is there a finite temperature or zero temperature ideal glass transition? In this case, is the transition of static or purely dynamic origin?
- Is there a geometric, real space explanation for the dynamic slowing down that takes into account molecular degrees of freedom?

The glass transition appears as a kind of ‘intermediate coupling’ problem, since for instance typical growing lengthscales are found to be at most a few tens of particle large close to T_g . It would therefore be difficult to recognize the correct theory even if one bumped into it. To obtain quantitative, testable predictions, one must therefore be able to work out also preasymptotic effects. This is particularly difficult, especially in cases where the asymptotic theory itself has not satisfactorily been worked out. As a consequence, at this time, theories can only be judged by their overall predictive power and their theoretical consistency.

A. Cooperativity, chaotic energy landscapes and Random First Order Theory

In the last two decades, three independent lines of research approaches, Adam-Gibbs theory [64], mode-coupling theory [31] and spin glass theory [65], have merged to produce a theoretical ensemble that now goes under the name of Random First Order Theory (RFOT), a terminology introduced by Kirkpatrick, Thirumalai and Wolynes [66] who played a major role in its development. Instead of following the rambling development of history, we summarize it in a more modern and unified way.

A key ingredient of RFOT is the existence of a chaotic or complex free energy landscape and its evolution with temperature and/or density. Analysing it in a controlled way for three dimensional interacting particles system is of course an impossible task. This can be achieved, however, in simplified models or using mean-field approximation, that have therefore played a crucial role in the development of RFOT.

A first, concrete example is given by ‘lattice glass models’ [67]. These are models containing hard particles sitting on the sites of a lattice. The Hamiltonian is infinite if there is more than one particle on a site or if the number of occupied neighbors of an occupied site is larger than a parameter, m , but the Hamiltonian is zero otherwise. Tuning the parameter m , or changing the type of lattice, in particular its connectivity, yields different models. Lattice glasses are constructed as simple stat-mech models to study the glassiness of hard sphere systems. The constraint on the number of occupied neighbors mimicks the geometric frustration [68] encountered when trying to pack hard spheres in three dimensions. Other models, which have a finite energy and, hence, are closer to molecular glass-formers, can be also constructed [69]. These models can be solved exactly on a Bethe lattice [179]. This reveals an astonishing physical behaviour [70]. In particular their free energy landscape can be analyzed in full details and turns out to have the properties that are also found in several ‘generalized spin glasses’.

Probably the most studied example of such spin glasses is the p -spin model, defined by the Hamiltonian [71]

$$H = - \sum_{i_1, \dots, i_p} J_{i_1, \dots, i_p} S_{i_1} \dots S_{i_p}, \quad (14)$$

where the S_i s are N Ising or spherical spins, $p > 2$ and J_{i_1, \dots, i_p} quenched random couplings with zero mean variance $p!/(2N^{p-1})$.

All these models (lattice glasses, their finite energy generalizations and their quenched disorder counterparts) belong to the class of one-step replica symmetry breaking systems [65]. This makes reference to the ansatz that is needed [71] when replica techniques are used to compute the thermodynamic behaviour of the model in Eq. (14). This corresponds to the universality class of chaotic (or random) free energy landscapes, as we now explain.

The free energy landscape of these systems is ‘rugged’, characterized by many minima and saddle points. Actually, the number of stationary points is so large that in order to count them one has to introduce an entropy, called configurational entropy or complexity, $s_c = \frac{1}{N} \log \mathcal{N}(f)$, where $\mathcal{N}(f)$ is the number of stationary points with a given free energy density f . The density profile corresponding to one given minimum is amorphous and lacks any type of periodic long-range order, and different minima are very different. Defining a similarity measure between them, an ‘overlap’, one typically finds that two minima with the same free energy f have zero overlap.

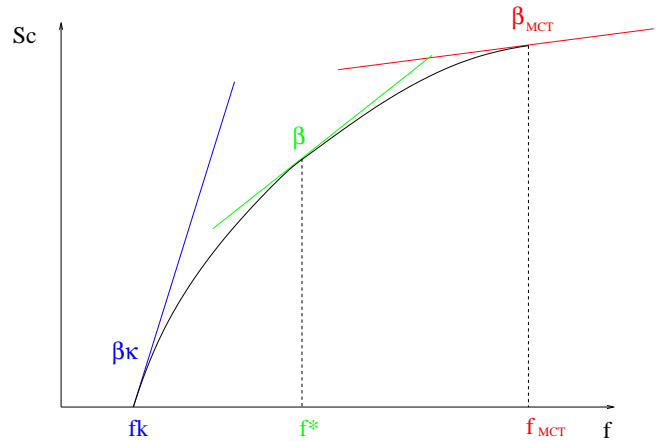


FIG. 13: Typical shape of the configurational entropy, s_c , as a function of free energy density, f in the range $T_k < T < T_{MCT}$ for random first order landscapes. A graphic solution of Eq. (16) is obtained by finding the value of f at which the slope of the curve is β . Note that s_c is also a function of temperature, so this curve in fact changes with T .

The typical shape of the configurational entropy as a function of f is plotted in Fig 13.

At high temperature, there is typically a single minimum, the high temperature liquid state. There is a temperature below which an exponentially large (in the system size) number of minima appears. Within mean-field models, corresponding to Bethe or completely connected lattices, these minima correspond to macroscopic physical states analogous to the periodic minimum corresponding to the crystal [180]. Once the system is in one of these states it remains trapped in it forever, since barriers separating states diverge with the system size. However, as explained below, when transposed to finite dimensional systems these states become metastable and have a finite lifetime. As a consequence, in order to compute thermodynamic properties, one has to sum over all of them using the Boltzmann weight $\exp(-\beta N f_\alpha)$ for each state α [72]:

$$Z = \sum_{\alpha} e^{-\beta N f_{\alpha}} = \int df \exp[N s_c(f; T)] e^{-\beta N f}, \quad (15)$$

where $\beta = 1/(K_B T)$. Evaluating this sum by saddle point method yields three regimes. At high temperature, $T > T_{MCT}$, the liquid corresponding to a flat density profile dominates the sum. The landscape is simple and has a single minimum. This is followed by an intermediate temperature regime, $T_k < T < T_{MCT}$, where the sum is dominated by all terms with free energy density satisfying

$$\left. \frac{\partial s_c(f, T)}{\partial f} \right|_{f=f^*} = \beta. \quad (16)$$

There are many of them, the logarithm of their number being given by $N s_c(f^*, T)$, see Fig. 13 for a graphical solution of Eq. (16). Upon decreasing the temperature,

$s_c(f^*, T)$ decreases until a temperature, T_K , below which the sum in Eq. (15) becomes dominated by only few terms corresponding to states with free energy density f_K given by $s_c(f_K, T) = 0$, see Fig. 13. The entropy in the intermediate temperature range above T_K has two contributions: the one counting the number of minima, given by s_c , and the intra-state entropy, s_{in} , counting the number configurations inside each state. At T_K , the configurational entropy vanishes, $s_c(T_K) = 0$. As a consequence the specific heat undergoes a jump towards a smaller value across T_K , an exact realization of the ‘entropy vanishing’ mechanism conjectured by Kauzmann [8].

Let us discuss the dynamical behaviour which results from the above analysis. We have already mentioned that relaxation processes do not occur below T_{MCT} because states have an infinite lifetime. The stability of these states can be analyzed by computing the free energy Hessian in the minima [73]. One finds that states become more fragile when $T \rightarrow T_{MCT}^-$, are marginally stable at $T = T_{MCT}$, unstable for $T > T_{MCT}$. The dynamics of these models can be analyzed exactly [74]. Coming from high temperature, the dynamics slows down and the relaxation time diverges at T_{MCT} in a power law manner,

$$\tau_\alpha \sim \frac{1}{(T - T_{MCT})^\gamma}, \quad (17)$$

where γ is a critical exponent. The physical reason is the incipient stable states that appear close to T_{MCT} . The closer the temperature is to T_{MCT} , the longer it takes to find an unstable direction to relax.

Amazingly, the dynamical transition that appears upon approaching T_{MCT} in random first order landscapes is completely analogous to the one predicted to occur in supercooled liquids by the Mode-Coupling Theory of the glass transition, and developed independently by Leuthesser, Bengtzelius, Götze, Sjölander and coworkers [31]. Actually, MCT can be considered as an approximation which becomes controlled and exact for these mean-field models. Originally, MCT was developed using projector operator formalism [76, 77] and field-theory methods [78] to yield closed integro-differential equations for the dynamical structure factor in supercooled liquids. These approaches were recently generalized [79, 80] to deal with dynamic heterogeneity and make predictions for the multi-point susceptibilities and correlation functions discussed in Sec. VI. Within MCT, the relaxation timescale diverge in a power law fashion at T_{MCT} , as in Eq. (17). This divergence is accompanied by critical behaviour that appears both in space (long range spatial dynamic correlations), and in time (power laws in time).

Comparing Eqs. (1) and (17) makes it clear that MCT cannot be used to describe viscosity data close to T_g since it does not predict activated behaviour. It is now recognized that an MCT transition at T_{MCT} does not occur in real materials, so that T_{MCT} is, at best, a dynamical crossover. A central advantage of MCT is that it can yield quantitative predictions from microscopic input ob-

tained for a particular material. As such it has been applied to yield predictions for scores of different systems that can be directly confronted to experimental or numerical measurements. A major drawback is the freedom offered by the ‘crossover’ nature of the MCT transition, so that ‘negative’ results can often be attributed to corrections to asymptotic predictions rather than deficiencies of the theory itself. Nevertheless, MCT continues to be studied, applied and generalized to study many different physical situations [31], including aging systems (see Sec. VIII), or non-linear rheology of glassy materials [81–83].

What happens below T_{MCT} in finite dimensional system if the relaxation time does not diverge as predicted in Eq. (17)? Why is the transition avoided? In fact, the plethora of states that one finds in mean-field are expected to become (at best) metastable in finite dimension, with a finite lifetime, even below T_{MCT} . What is their typical lifetime, and how these metastable states are related to the structural relaxation are issues that still await for a complete microscopic analysis.

There exist, however, phenomenological arguments [59, 84, 85], backed by microscopic computations [86, 87] that yield a possible solution dubbed ‘mosaic state’ by Kirkpatrick, Thirumalai and Wolynes [84]. Schematically, the mosaic picture states that, in the regime $T_K < T < T_{MCT}$, the liquid is composed of domains of linear size ξ . Inside each domain, the system is in one of the mean-field states. The length of the domains is fixed by a competition between energy and configurational entropy. A state in a finite but large region of linear size l can be selected by appropriate boundary conditions that decrease its free energy by an amount which scales as Υl^θ with $\theta \leq 2$. On the other hand, the system can gain entropy, which scales as $s_c l^3$, if it visits the other numerous states. Entropy obviously gains on large lengthscales, the crossover length ξ being obtained by balancing the two terms,

$$\xi = \left(\frac{\Upsilon}{T s_c(T)} \right)^{1/(3-\theta)}. \quad (18)$$

In this scenario, the configurational entropy on scales smaller than ξ is too small to stir the configurations efficiently and win over the dynamically generated pinning field due to the environment, while ergodicity is restored at larger scale. Hence, the relaxation time of the system is the relaxation time, $\tau(\xi)$, of a finite size regions of the system. Barriers are finite, unlike in the mean-field treatment. Smaller length scales are faster but unable to decorrelate, whereas larger scales are orders of magnitude slower. Assuming thermal activation over energy barriers which are supposed to grow with size as ξ^ψ , one predicts finally, using Eq. (18), that

$$\log \left(\frac{\tau_\alpha}{\tau_0} \right) = c \frac{\Upsilon}{k_B T} \left(\frac{\Upsilon}{T s_c(T)} \right)^{\psi/(3-\theta)}, \quad (19)$$

where c is a constant.

The above argument is rather generic and therefore not very predictive. Recently, microscopic computations [86, 87] have been performed with the aim of putting these phenomenological arguments on a firmer basis and computing the exponents θ and ψ . The results are unfortunately not yet conclusive because they involve replica calculations with uncontrolled assumptions, but they do confirm the phenomenological scenario presented above and suggest that $\theta = 2$. Some other phenomenological arguments suggest the value of $\theta = 3/2$ [84]. There are no computation available for ψ , only the suggestion that $\psi = \theta$ [84].

Note that using the value $\theta = 3/2$ with $\theta = \psi$ simplifies Eq. (19) into a form that is well-known experimentally and relates $\log \tau_\alpha$ directly to $1/S_c$, which is the celebrated Adam-Gibbs relation [64] between relaxation time and configurational entropy that is in rather good quantitative agreement with many experimental results [88–90]. The Random First Order Theory can be considered, therefore, as a microscopic theory that reformulates and generalizes the Adam-gibbs mechanism. Furthermore, using the fact that the configurational entropy vanishes linearly at T_K one predicts also a VFT divergence of the relaxation time as in Eq. (1), with the identification that

$$T_0 = T_K. \quad (20)$$

The equality (20) between two temperatures that are commonly used in the description of experimental data certainly constitutes a central achievement of RFOT since it accounts for the empirical relation found between the kinetics and the thermodynamics of supercooled liquids. Furthermore RFOT naturally contains MCT, which can be used to describe the first decades of the dynamical slowing down, while the spin glass side of RFOT qualitatively explains the dynamics in terms of the peculiar features of the free energy landscape that have been detailed above. Dynamics first slows down because there appear incipient metastable states, and once this metastable states are formed, the dynamics becomes dominated by the thermally activated barrier crossing from one metastable state to another, which is consistent with the relation between dynamical correlation length and timescale discussed in Sec. VI. Quite importantly, microscopic computations of T_{MCT} and T_0 for realistic models of liquids are possible [91, 92]. This is a most desirable feature, even if the results are not very accurate [93–95].

Probably the most serious weakness of the RFOT construction is that the theory, although worked out in full details within mean-field models, has remained elusive for finite dimensional systems, for which it has a still speculative flavour. Worrying is the fact that no simple three-dimensional glassy model, let alone interacting particles in the continuum, has been discovered yet, for which this theory has been shown to apply. Furthermore the entropy driven nucleation theory that leads to the VFT law is not understood completely. Although the ul-

timate consequences of the theory are sometimes in very good agreement with experiments, as Eq. (20), the conclusion that RFOT is correct is premature. In fact direct tests of the mosaic state picture are rare, and not conclusive yet [96]. We hope that in the next few years, joint theoretical and experimental efforts will drive RFOT into a corner, to a point where it can be decided whether or not it is a valid theory for the glass transition.

B. Free volume, defects, and facilitated models

In this subsection we motivate and briefly summarize studies of a different family of statistical mechanics models that turns out to yield a rich variety of physical behaviours. Their starting point are physical assumptions that might seem similar to the models described in Sec. VII A, but the outcome yields a different physical explanation of the glass transition. Although the two theoretical approaches cannot be simultaneously correct, they both have been influential and very instructive in order to develop a theoretical understanding of glassy phenomena. Furthermore, despite the ‘great unification’ phase diagram in Fig. 4, it could be that glass and jamming transitions in colloids, granular media and glass-formers have a different nature, so that different theories could apply to different phenomena.

As in Sec. VII A, we start from the packing considerations that are more appropriate for hard spheres systems. We follow first Kob and Andersen [97] and again use a lattice gas description of the physics and work on a three dimensional cubic lattice. As in a hard sphere system, we assume no interaction between particles beyond the hard-core constraint that the occupation number n_i at site i is at most equal to 1,

$$H[\{n_i\}] = 0, \quad n_i = 0, 1. \quad (21)$$

Contrary to the lattice glass model presented above, all configurations respecting the hard-core constraint are allowed and are equally probable. Geometric frustration is instead introduced at the level of the kinetic rules, that are defined as constrained local moves. Namely, a particle can jump to a nearest neighbor site only if that site is empty (to satisfy the hard-core constraint), but, additionally, only if the sites occupied before and after the move have less than m neighbors, m being an adjustable parameter, which Kob and Andersen choose as $m = 4$ for $d = 3$ ($m = 6$ corresponds to the unconstrained lattice gas). The model captures the idea that if the liquid is locally very dense, no movement is possible while regions with low density move more easily.

Of course, such kinetically constrained lattice gases have been studied in various spatial dimensions, for different values of m , for different constraints, or even different lattice geometries [98]. They can be thought of as models capturing the idea of a ‘cage’ effect in a strict sense, utilizing the notion that a particle with a dense neighbor shell cannot diffuse. Although the cage seems

a purely local concept, it turns out that diffusion in constrained lattice gases arises from cooperative rearrangements, so that slow dynamics can be directly shown to be driven by the growth of dynamic lengthscales for these cooperative moves [99–101]. This strongly suggests that such cooperative moves are most probably at work also in real liquids.

In this lattice gas picture, the connection with liquid is not obvious because density (‘free volume’), rather than temperature controls the dynamics. Thermal models with similar features can in fact be defined along the following lines. In a liquid, low temperature implies a very small probability to find a location with enough free volume to move. The idea of a small concentration of ‘hot spots’ is in fact reminiscent of another picture of the glass transition based on the idea of ‘defects’ which is captured by the defect model proposed by Glarum [102] in the 60’s, where relaxation proceeds via the diffusion of a low concentration of independent defects. In the mid-80’s, using the conjugated ideas of kinetic constraints and rare defects, Fredrickson and Andersen defined a family of kinetic Ising models for the glass transition [103]. They study an assembly of non-interacting spins,

$$H[\{n_i\}] = \sum_{i=1}^N n_i, \quad n_i = 0, 1, \quad (22)$$

where $n_i = 1$ represent the defects, whose concentration becomes exponentially small at low temperature, $\langle n_i \rangle \approx \exp(-1/T)$. As for the Kob-Andersen lattice gas, the non-trivial ingredient lies in the chosen rates for the transition between states. The kinetic rules stipulate that a transition at site i can happen with a usual Glauber rates, but only if site i is surrounded by at least k defects ($k = 0$ corresponds to the unconstrained limit). Again, one can easily imagine studying such models in different spatial dimensions, on different lattices, and with slightly different kinetic rules, yielding a large number of possible behaviours [98, 104]. The similarity between those spin facilitated models and the kinetically constrained lattice gases is striking. Altogether, they form a large family of models generically called kinetically constrained models (KCMs) [98].

The connection between KCMs and the much older concept of free volume is obvious from our presentation. Free volume models are among the most widely used models to analyze experimental data, especially in polymeric systems. They have been thoroughly reviewed before [10, 105], and the main prediction is that dynamic slowing down occurs because the free volume available to each particle, v_f , vanishes at some temperature T_0 as $v_f \approx \alpha(T - T_0)$, a relation which connects volume to temperature. Statistical arguments then relate relaxation timescales to free volume assuming that movement is possible if locally there is ‘enough’ free volume available, more than a typical value v_0 . This is clearly reminiscent of the above idea of a kinetic constraint for local moves in lattice gases. An appealing VFT divergence is

then predicted:

$$\frac{\tau_\alpha}{\tau_0} \sim \exp\left(\gamma \frac{v_0}{v_f}\right) \sim \exp\left(\frac{\gamma v_0/\alpha}{[T - T_0]^\mu}\right), \quad (23)$$

where γ is a numerical factor and $\mu = 1$. Predictions such as Eq. (23) justify the wide use of free volume approaches, despite the many (justified) criticisms that have been raised.

Initially it was suggested that KCMs would similarly display finite temperature or finite density dynamic transitions similar to the one predicted by the mode-coupling theory of supercooled liquids [103], but it was soon realized [106, 107] that most KCMs do not display such singularity, and timescales in fact only diverge in the limit of zero temperature ($T = 0$) or maximal density ($\rho = 1$). Recently, models displaying a $T_c > 0$ or $\rho_c < 1$ transition have been introduced and analyzed [108]. They provide a microscopic realization, based on well-defined statistical mechanics models, of the glass transition predicted by free volume arguments. Their relaxation timescale diverges with a VFT-like form but with an exponent $\mu \simeq 0.64$. Understanding their universality classes and how general is the mechanism leading to the transition is still an open problem.

Extensive studies have shown that KCMs have a macroscopic behaviour which resembles the phenomenology of supercooled liquids, displaying in particular Arrhenius or super-Arrhenius increase of relaxation timescales on decreasing the temperature and non-exponential relaxation functions at equilibrium [98]. Early studies also demonstrated that, when suddenly quenched to very low temperatures, the subsequent non-equilibrium aging dynamics of the models compares well with experimental observations on aging liquids [106]. Moreover, the many possibilities to define the models mean that they might exhibit a broad variety of possible behaviours. This is both a positive and a negative aspect: on the one hand one can explore various scenarii to describe glass transition phenomena, but on the other hand, one would like to be able to decide what particular model should be used if one wants to get a predictive quantitative description for a particular liquid. In fact, contrary to MCT, no microscopic calculations have been performed using the framework of KCMs. Rather than predicting the quantitative behaviour of a material in all its microscopic details, it is perhaps more appropriate to use KCMs as theoretical tools to define concepts and obtain new ideas.

It is precisely in this perspective that interest in KCMs continues to increase, in large part since it was realized that their dynamics is spatially heterogeneous [37, 99, 107], a central feature of supercooled liquids dynamics. It is only fair to say that in-depth studies of KCMs have greatly contributed to our theoretical understanding of the spatially heterogeneous dynamics in glass and jamming problems. Remarkably, virtually all the aspects related to dynamic heterogeneity mentioned in Sec. VI can be investigated and rationalized, at least qualitatively, in terms of KCMs. The dynam-

ics of these systems can be understood in terms of defects motion [98]. Depending on the particular model, defects can diffuse or have a more complicated motion. Furthermore, they can simply be point-like, or ‘cooperative’ (formed by point-like defects moving in a cooperative way). A site can relax when it is visited by a defect. As a consequence, the heterogeneous character of the dynamics is entirely encoded in the defect configuration and defect motion [37, 48]. For instance, a snapshot similar to Fig. 7 in a KCM shows clusters which have relaxed within the time interval t [109, 110]. These are formed by all sites visited by a defect between 0 and t . The other sites are instead frozen in their initial state. In these models the dynamics slows down because the defect concentration decreases. As a consequence, in the regime of slow dynamics there are few defects and strong dynamic heterogeneity. Detailed numerical and analytical studies have indeed shown that in these systems, non-exponential relaxations patterns do stem from a spatial, heterogeneous distribution of timescales, directly connected to a distribution of dynamic lengthscales [37, 100, 101, 108, 109, 111]. Decoupling phenomena appear in KCMs and can be shown to be very direct, quantifiable, consequences of the dynamic heterogeneity [45], which also deeply affects the process of self-diffusion in a system close to its glass transition [112]. More fundamentally, multi-point susceptibilities, multi-point spatial correlation functions such as the ones defined in Eqs. (8) and (11) can be studied in much greater detail than in molecular systems, to the point that scaling relations between timescales, lengthscales, and dynamic susceptibilities can be established [36, 48, 101, 113, 114]. This type of scaling behaviour has been observed close to $T = 0$ and $\rho = 1$ in spin models and lattice gases without a transition [181]. These particular points of the phase diagram have been shown, by various theoretical means, to correspond to true critical points where timescales and dynamic lengthscales diverge with well-defined critical laws [111, 114]. Such ‘dynamic criticality’ is a useful concept because it implies the possibility that some universal behaviour emerges in the physics of supercooled liquids, precisely of the type observed in Fig. 12.

A central criticism about the free volume approach, that is equally relevant for KCMs concerns the identification, at the molecular level, of the vacancies (in lattice gases), mobility defects (in spin facilitated models), or free volume itself. Attempts to provide reasonable coarse-graining from molecular models with continuous degrees of freedom to lattice models with kinetic rules are so far very limited, and not really convincing [53, 115]. On the other hand the proof that kinetic rules can emerge effectively and induce a slow dynamics has been obtained for simple lattice spin models [116], whose dynamics directly maps onto constrained models. Several examples are available but here we only mention the simple case of the bidimensional plaquette model defined by a Hamiltonian of a p -spin type, but in two dimensions on a square

lattice of linear size L ,

$$H = -J \sum_{i=1}^{L-1} \sum_{j=1}^{L-1} S_{i,j} S_{i+1,j} S_{i,j+1} S_{i+1,j+1}, \quad (24)$$

where $S_{i,j} = \pm 1$ is an Ising variable lying at node (i, j) of the lattice. Contrary to KCMs, the Hamiltonian in Eq. (24) contains genuine interactions, which are no less (or no more) physical than p -spin models discussed in Sec. VII A. Interestingly the dynamics of this system is (trivially) mapped onto that of a KCM by analyzing its behaviour in terms of plaquette variables, $p_{i,j} \equiv S_{i,j} S_{i+1,j} S_{i,j+1} S_{i+1,j+1}$, such that the Hamiltonian becomes a non-interacting one, $H = -J \sum_{i,j} p_{i,j}$, as in Eq. (22). More interestingly, the analogy also applies to the dynamics [116]. The fundamental moves are spin-flips, but when a single spin is flipped the states of the four plaquettes surrounding that spin change. Considering the different types of moves, one quickly realizes that excited plaquettes, $p_{i,j} = +1$, act as sources of mobility, since the energetic barriers to spin flips are smaller in those regions. This observation allows to identify the excited plaquettes as defects, by analogy with KCMs. Spatially heterogeneous dynamics, diverging lengthscales accompanying diverging timescales and scaling behaviour sufficiently close to $T = 0$ can be established by further analysis [117], providing a simple, but concrete example, of how an interacting many body system might effectively behave as a model with kinetic constraints [182].

Another essential drawback of facilitated models is that among the microscopic ‘details’ thrown away to arrive at simple statmech models such as the ones in Eqs. (21) and (22), information on the thermodynamic behaviour of the liquids has totally disappeared. In particular, a possible coincidence between VFT and Kauzmann temperatures, T_0 and T_K is not expected, nor can the dynamics be deeply connected to thermodynamics, as in Adam-Gibbs relations. The thermodynamic behaviour of KCMs appears different from the one of real glass-formers close to T_g [120]. This is probably the point where KCMs and RFOT approaches differ more evidently. Even though the dynamics of KCMs shares similarities with systems characterized with a complex energy landscape [122, 123], thermodynamical behaviours are widely different in both cases, as has been recently highlighted in Ref. [124] by focusing on the concrete examples of plaquette models such as in Eq. (24).

Finally, when KCMs were first defined, they were argued to display a dynamic transition of a nature very similar to the one predicted by MCT [103]. Although the claim has been proven wrong [183], it bears some truth: both approaches basically focus on the kinetic aspects of the glass transition and they both predict the existence of some dynamic criticality with diverging lengthscales and timescales. This similarity is even deeper, since a mode-coupling singularity is truly present when (some) KCMs are studied on the Bethe lattice [100, 121], but is ‘avoided’ when more realistic lattice geometries are con-

sidered. This underlies the similarity of these two approaches while emphasizing further the mean-field character of the MCT approach.

C. Geometric frustration, avoided criticality, and Coulomb frustrated theories

In all of the above models, ‘real space’ was present in the sense that special attention was paid to different lengthscales characterizing the physics of the models that were discussed. However, apart from the ‘packing models’ with hard-core interactions, no or very little attention was paid to the geometric structure of local arrangements in molecular liquids close to a glass transition. This slight ‘oversight’ is generally justified using concepts such as ‘universality’ or ‘simplicity’, meaning that one studies complex phenomena using simple models, a typical statistical mechanics perspective. However, important questions remain: what is the liquid structure within mosaic states? How do different states differ? What is the geometric origin of the defects invoked in KCMs? Are they similar to defects (disclinations, dislocations, vacancies, etc.) found in crystalline materials?

There exists a line of research in this field which attempts to provide answers to these questions. It makes heavy use of the concept of geometric frustration. Broadly speaking, frustration refers to the impossibility of simultaneously minimizing all the interaction terms in the energy function of the system. Frustration might arise from quenched disorder (as in the spin glass models described above), but liquids have no quenched randomness. In that case, frustration has a purely geometric origin. It is attributed to a competition between a short-range tendency for the extension of a ‘locally preferred order’, and global constraints that prevent the periodic tiling of space with this local structure.

This can be illustrated by considering once more the packing problem of spheres in three dimensions. In that case, the locally preferred cluster of spheres is an icosahedron. However, the 5-fold rotational symmetry characteristic of icosahedral order is not compatible with translational symmetry, and formation of a periodic icosahedral crystal is impossible [125]. The geometric frustration that affects spheres in three dimensional Euclidean space can be relieved in curved space [68]. In Euclidian space, the system possesses topological defects (disclination lines), as the result of forcing the ideal icosahedral ordering into a ‘flat’ space. Nelson and coworkers have developed a solid theoretical framework based on this picture to suggest that the slowing down of supercooled liquids is due to the slow wandering of these topological defects [68], but their treatment remains so complex that few quantitative, explicit results have been obtained.

This picture of sphere packing disrupted by frustration has been further developed in simple statistical models characterized by geometric frustration, in a pure statistical mechanics approach [61]. To build such a model,

one must be able to identify, then capture, the physics of geometric frustration. Considering a locally ordered domain of linear size L , Kivelson *et al.* [126] suggest that the corresponding free energy scales as

$$F(L, T) = \sigma(T)L^2 - \phi(T)L^3 + s(T)L^5, \quad (25)$$

The first two terms express the tendency of growing local preferred order and they represent respectively the energy cost of having an interface between 2 phases and a bulk free energy gain inside the domain. Geometric frustration is encoded in the third term which represents the strain free energy resulting from the frustration. The remarkable feature of Eq. (25) is the super-extensive scaling of the energy cost due to frustration which opposes the growth of local order. The elements in Eq. (25) can then be directly incorporated into ferromagnetic models where ‘magnetization’ represents the local order, ferromagnetic interactions the tendency to local ordering, and Coulombic antiferromagnetic interactions the opposite effect of the frustration. The following Hamiltonian possesses these minimal ingredients:

$$H = -J \sum_{\langle i, j \rangle} \mathbf{S}_i \cdot \mathbf{S}_j + K \sum_{i \neq j} \frac{\mathbf{S}_i \cdot \mathbf{S}_j}{|\mathbf{x}_i - \mathbf{x}_j|}, \quad (26)$$

where the spin \mathbf{S}_i occupies the site i at position \mathbf{x}_i . Such Coulomb frustrated models have been studied in great detail, using various approximations to study models for various space and spin dimensions [61].

The general picture is that the ferromagnetic transition occurring at $T = T_c^0$ in the pure model with no frustration, $K = 0$, is either severely depressed to lower temperatures for $K > 0$, sometimes with a genuine discontinuity at $K \rightarrow 0$, yielding the concept of ‘avoided criticality’. For the simple case of Ising spins in $d = 3$, the situation is different since the second order transition becomes first order between a paramagnetic phase and a spatially modulated phase (stripes). For $K > 0$ and $T < T_c^0$ the system is described as a ‘mosaic’ of domains corresponding to some local order, whose size increases (but does not diverge!) when T decreases. Tarjus, Kivelson and co-workers clearly demonstrate that such a structuration into mesoscopic domains allows one to understand most of the fundamental phenomena occurring in supercooled liquids [61]. Their picture as a whole is very appealing because it directly addresses the physics in terms of the ‘real space’, and the presence of domains of course connects to ideas such as cooperativity, dynamic heterogeneity and spatial fluctuations, that directly explains, at least qualitatively, non-exponential relaxation, decoupling phenomena or super-Arrhenius increase of the viscosity. However, as for the RFOT mosaic picture, direct confirmations of this scenario are rare [127]. Icosahedral order has not been clearly linked to the dynamics of hard spheres, while the very notion of local order in more realistic glass-forming liquids (such binary mixtures of spheres, or larger molecules with internal degrees of freedom) is problematic and not easily defined. This makes

the basis of the scenario very fragile, and its practical applicability for a particular material difficult.

VIII. AGING AND OFF-EQUILIBRIUM

A. Why aging?

We have dedicated most of the above discussion to properties of materials approaching the glass transition at thermal equilibrium. We discussed a rich phenomenology and serious challenges for both our numerical and analytical capabilities to account for these phenomena. For most people, however, glasses are interesting below the glass transition, so deep in the glass phase that the material seems to be frozen forever in a seemingly arrested amorphous state, endowed with enough mechanical stability for a glass to retain, say, the liquid it contains (preferentially a nice red wine). Does this mean that there is no interesting physics in the glass state?

The answer is clearly ‘no’. There is still life (and physics) below the glass transition. We recall that for molecular glasses, T_g is defined as the temperature below which relaxation is too slow to occur within an experimental timescale. Much below T_g , therefore, the equilibrium relaxation timescale is so astronomically large that thermal equilibrium is out of reach. One enters therefore the realm of off-equilibrium dynamics. A full physical understanding of the non-equilibrium glassy state remains a central challenge [4, 75].

A first consequence of studying materials in a time window smaller than equilibrium relaxation timescales is that the system can, in principle, remember its complete history, a most unwanted experimental situation since all details of the experimental protocol may then matter. The simplest protocol to study aging phenomena in the glass phase is quite brutal [3]: take a system equilibrated above the glass transition and suddenly quench it at a low temperature at a ‘waiting time’ $t_w = 0$ which corresponds to the beginning of the experiment. For $t_w > 0$ the system is left unperturbed at constant temperature where it tries to slowly reach thermal equilibrium, even though it has no hope to ever get there. Aging means that the system never forgets the time t_w spent in the glass phase, its ‘age’. This is illustrated in Fig. 14 where the self-part of the intermediate function in Eq. (5) is shown for a Lennard-Jones molecular liquid at low temperature. Immediately after the quench, the system exhibits a relatively fast relaxation: particles still move substantially. However, when the age of the system increases, dynamics slows down and relaxation becomes much slower. When t_w becomes very large, relaxation becomes too slow to be followed in the considered time window and the system seems frozen on that particular timescale: it has become a glass.

A popular interpretation of this phenomenon is given by considering trap models [128]. In this picture, reminiscent of the Goldstein view of the glass transition men-

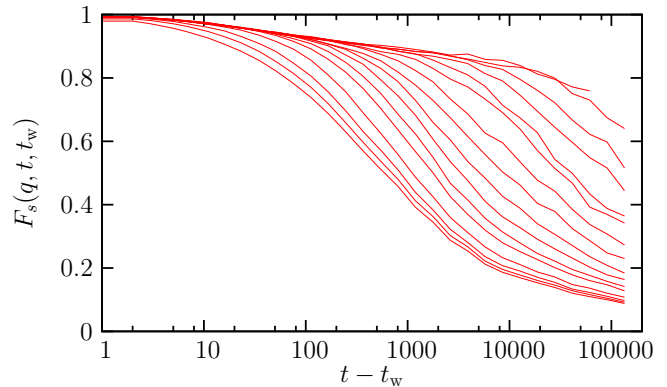


FIG. 14: Aging dynamics in a Lennard-Jones glass-forming liquid at low temperature. The system is quenched at time $t_w = 0$ at low T , where the temperature is kept constant. Two-time self-intermediate scattering functions are then measured for 20 logarithmically spaced waiting times t_w from $t_w = 1$ to $t_w = 10^5$ (from left to right). The relaxation becomes slower when t_w increases: the system ages.

tioned above [9], the system is described as a single particle evolving in a complex energy landscape with a broad distribution of trap depths—a paradigmatic mean-field approach. Aging in this perspective arises because the system visits traps that are increasingly deep when t_w increases, corresponding to more and more stable states. It takes therefore more and more time for the system to escape, and the dynamics slows down with time, as observed in Fig. 14. This implies that any physical property of the glass becomes an age-dependent quantity in aging protocols, and more generally dependent on how the glass was prepared. One can easily imagine using this property to tune mechanical or optical characteristics of a material by simply changing the way it is prepared, like how fast it is cooled to the glassy state.

A real space alternative picture was promoted in particular in the context of spin glass studies, based on the ideas of scaling and renormalization [129, 130]. The physical picture is that of a coarsening process, where the system develops long-range order by growing extended domains of lengthscale $\ell(t_w)$. On lengthscales less than $\ell(t_w)$ the system has ordered since the quench at $t_w = 0$. The domain walls evolve in a random environment. In order to move they have to overcome free energy barriers. It is then assumed an activated dynamic scaling which states that the typical barrier to extend the domain from linear size $\ell(t_w)$ to, say, $2\ell(t_w)$ scales as ℓ^ψ , where ψ is some ‘barrier’ exponent. Using the Arrhenius law to relate dynamics to barriers, one gets that aging corresponds to the logarithmic growth with time of spatially correlated domains, $\ell \sim (T \log t_w)^{1/\psi}$. A domain growth picture of aging in spin glasses can be directly confirmed by numerical simulations [131], only indirectly by experiments.

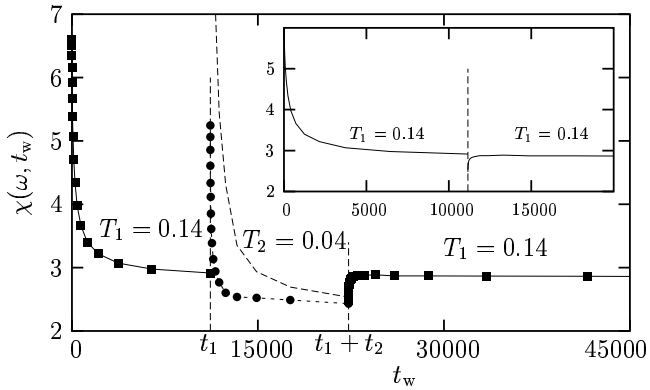


FIG. 15: Memory and rejuvenation effects obtained in the numerical simulation of a three-dimensional Heisenberg spin glass. There is a first aging step, $0 < t_w < t_1$, during which the system slowly tries to reach thermal equilibrium at temperature T_1 . The system ‘rejuvenates’ in the second step at T_2 , $t_1 < t < t_1 + t_2$, and it restarts aging (rejuvenation). Finally in the third step, temperature is back to T_1 , and memory of the first step is kept intact, as shown in the inset where relaxation during the second step of the experiment is taken away.

B. Memory and rejuvenation effects

Since the complete history of a sample in the glass phase matters, there is no reason to restrain experimental protocols to the simple aging experiment mentioned above. Indeed, experimentalists have investigated scores of more elaborated protocols that have revealed an incredibly rich, and sometimes quite unexpected, physics [4]. We restrain ourselves here to a short discussion of memory and rejuvenation effects observed during temperature cycling experiments [132] (one can imagine applying a magnetic field or a mechanical constraint, be they constant in time or sinusoidal, etc.). These two effects were first observed in spin glasses, but the protocol was then repeated in many different materials, from polymers and organic liquids to disordered ferroelectrics. After several unsuccessful attempts, similar effects are now observed in numerical work as well. Results obtained from simulations of a three-dimensional Heisenberg spin glass [133] are presented in Fig. 15.

There are three steps in temperature cycling experiments [132]. The first one is a standard aging experiment, namely a sudden quench from high to low temperature at time $t_w = 0$. The system then ages for a duration t_1 at constant temperature T_1 . The system slowly relaxes towards equilibrium and its dynamics slows down, as observed in our spin glass example in Fig. 15 through the measurement of the magnetic susceptibility $\chi(\omega, t_w)$. Temperature is then suddenly shifted to $T_2 < T_1$ at time t_1 . There, the material restarts aging (almost) as if the first step had not taken place. This is called ‘rejuvenation effect’, because the system seems to forget it is already

‘old’. At total time $t_1 + t_2$, temperature is then shifted back to its initial value T_1 . Then, aging is found to proceed as a quasi-perfect continuation of the first step, as if the second step had not taken place. The system has kept the ‘memory’ of the first part of the experiment, despite the rejuvenation observed in the intermediate part. The memory effect becomes more spectacular when relaxation during the second step is removed, as in the inset of Fig. 15. The third relaxation appears indeed as a perfect continuation of the first one.

On top of being elegant and quite intriguing, such protocols are relevant because they probe more deeply the dynamics of aging materials, allowing one to ask more precise questions beyond the simplistic observation that ‘this material displays aging’. Moreover, the observation of similar effects in many different glassy materials implies that these effects are intrinsic to systems with slow dynamics. Interesting also are the subtle differences observed from one material to the other.

Several experimental, numerical and theoretical papers have been devoted to this type of experiments, and these effects are not ‘mysterious’ anymore [134]. A clear link between memory effects and typical lengthscales over which the slow dynamics takes place has been established. Because lengthscales depend so sensitively on timescales and on the working temperature, experiments performed at two different temperatures typically probe very different lengthscales, allowing the system to store memory of its state at different temperatures at different lengthscales [135, 136]. In return, this link has been elegantly exploited to obtain a rather precise experimental estimate of dynamic lengthscales involved in the aging dynamics of spin glass materials [137], which seems to confirm the slow logarithmic growth law mentioned before.

Discussion of the rejuvenation effect is slightly more subtle. It is indeed not yet obvious that the effect as it is observed in computer simulations and reported, e.g., in Fig. 15 is exactly similar to the one observed in experiments. The difficulty comes from the fact that some seemingly innocuous details of the experimental protocol, such as the necessary use in experiments of finite cooling rates, in fact play a crucial role and influence the physics so that direct comparison between experiments and simulations is difficult. In numerical work, rejuvenation can be attributed to a gradual change with temperature of the nature of spatial correlations between spins that develop with time [133, 136]. More drastic changes are predicted to occur in disordered systems as a result of the chaotic evolution with temperature of the metastable states in a spin glass (so-called ‘chaos effect’ [138]), that could also be responsible for the observed rejuvenation effect [139]. This scenario can be directly discarded in simulations, where spatial correlations can be easily measured and chaos sought (in vain) in a very direct manner. Understanding the very origin of the rejuvenation effect observed in experiments remains, however, a challenge.

C. Mean-field aging and effective temperatures

Theoretical studies of mean-field glassy models have provided important insights into the aging dynamics of both structural and spin glasses [140–142]. Although such models are defined in terms of spin degrees of freedom interacting via infinite-ranged interactions, the deep connections between them and the mode-coupling theory of the glass transition make them serious candidates to investigate glassy states in general, not only thermodynamic properties at thermal equilibrium but also non-equilibrium aging dynamics. Despite their often reported ‘simplicity’, it took several years to derive a proper asymptotic solution of the long-time dynamics for a series of mean-field spin glasses [74]. These results have then triggered an enormous activity [143] encompassing theoretical, numerical and also experimental work trying to understand further these results, and to check in more realistic systems whether they have some reasonable range of applicability beyond mean-field. This large activity, by itself, easily demonstrates the broad interest of these results.

In these mean-field models, thermal equilibrium is never reached, and aging proceeds by downhill motion in an increasingly flat free energy landscape [144], with subtle differences between spin glass and structural glass models. In both cases, however, time translational invariance is broken, and two-time correlation and response functions depend on both their time arguments. In fact, the exact dynamic solution of the equations of motion for time correlators displays behaviours in strikingly good agreement with the numerical results reported in Fig. 14.

In these systems, the equations of motion in the aging regime involve not only time correlations, but also time-dependent response functions. At thermal equilibrium response and correlations are not independent, since the fluctuation-dissipation theorem (FDT) relates both quantities. In aging systems, there is no reason to expect the FDT to hold and both quantities carry, at least in principle, distinct physical information. Again, the asymptotic solution obtained for mean-field models quantitatively establishes that the FDT does not apply in the aging regime. Unexpectedly, the solution also shows that a generalized form of the FDT holds at large waiting times [140]. This is defined in terms of the two-time connected correlation function for some generic observable $A(t)$,

$$C(t, t_w) = \langle A(t)A(t_w) \rangle - \langle A(t) \rangle \langle A(t_w) \rangle, \quad (27)$$

with $t \geq t_w$, and the corresponding two-time (impulse) response function

$$R(t, t_w) = T \left. \frac{\delta \langle A(t) \rangle}{\delta h(t_w)} \right|_{h=0}. \quad (28)$$

Here h denotes the thermodynamically conjugate field to the observable A so that the perturbation to the Hamiltonian (or energy function) is $\delta E = -hA$, and angled

brackets indicate an average over initial conditions and any stochasticity in the dynamics. Note that we have absorbed the temperature T in the definition of the response, for convenience. The associated generalized FDT reads then

$$R(t, t_w) = X(t, t_w) \frac{\partial}{\partial t_w} C(t, t_w), \quad (29)$$

with $X(t, t_w)$ the so-called fluctuation-dissipation ratio (FDR). At equilibrium, correlation and response functions are time translation invariant, depending only on $\tau = t - t_w$, and equilibrium FDT imposes that $X(t, t_w) = 1$ at all times. A parametric fluctuation-dissipation (FD) plot of the step response or susceptibility

$$\chi(t, t_w) = \int_{t_w}^t dt' R(t, t'), \quad (30)$$

against

$$\Delta C(t, t_w) = C(t, t) - C(t, t_w), \quad (31)$$

is then a straight line with unit slope. These simplifications do not occur in non-equilibrium systems. But the definition of an FDR through Eq. (29) becomes significant for aging systems [140, 141]. In mean-field spin glass models the dependence of the FDR on both time arguments is only through the correlation function,

$$X(t, t_w) \sim X(C(t, t_w)), \quad (32)$$

valid at large wait times, $t_w \rightarrow \infty$. For mean-field structural glass models, the simplification (32) is even more spectacular since the FDR is shown to be characterized by only two numbers instead of a function, namely $X \sim 1$ at short times (large value of the correlator) corresponding to a quasi-equilibrium regime, with a crossover to a non-trivial number, $X \sim X^\infty$ for large times (small value of the correlator). This implies that parametric FD plots are simply made of two straight lines with slope 1 and X^∞ , instead of the single straight line of slope 1 obtained at equilibrium.

Since any kind of behaviour is in principle allowed in non-equilibrium situations, getting such a simple, equilibrium-like structure for the FD relations is a remarkable result. This immediately led to the idea that aging systems might be characterized by an effective thermodynamic behaviour and the idea of quasi-equilibration at different timescales [145, 146]. In particular, generalized FD relations suggest to define an effective temperature, as

$$T_{\text{eff}} = \frac{T}{X(t, t_w)}, \quad (33)$$

such that mean-field glasses are characterized by a unique effective temperature, $T_{\text{eff}} = T/X^\infty$. It is thought of as the temperature at which slow modes are quasi-equilibrated. One finds in general that $0 < X^\infty < 1$,

such that $T_{\text{eff}} > T$, as if the system had kept some memory of its high temperature initial state.

The name ‘temperature’ for the quantity defined in Eq. (33) is not simply the result of a dimensional analysis but has a deeper, physically appealing meaning that is revealed by asking the following questions. How does one measure temperatures in a many-body system whose relaxation involves well-separated timescales? What is a thermometer (and a temperature) in a far from equilibrium aging material? Answers are provided in Refs. [145, 147] both for mean-field models and for additional toy models with multiple relaxation timescales. The idea is to couple an additional degree of freedom, such as a harmonic oscillator, $x(t)$, which plays the role of the thermometer operating at frequency ω , to an observable of interest $A(t)$ via a linear coupling, $-\lambda x(t)A(t)$. Simple calculations show then that the thermometer ‘reads’ the following temperature,

$$\frac{1}{2}K_B T_{\text{meas}}^2 \equiv \frac{1}{2}\omega^2 \langle x^2 \rangle = \frac{\omega C'(\omega, t_w)}{2\chi''(\omega, t_w)}, \quad (34)$$

where $C'(\omega, t_w)$ is the real part of the Fourier transform of Eq. (27), and $\chi(\omega, t_w)$ the imaginary part of the Fourier transform of Eq. (28), with $h = \lambda x$. The relation (34) indicates that the bath temperature is measured, $T_{\text{meas}} = T$, if frequency is high and FDT is satisfied, while $T_{\text{meas}} = T_{\text{eff}} > T$ if frequency is slow enough to be tuned to that of the slow relaxation in the aging material. The link between the FDR in Eq. (29) and the effective temperature measured in Eq. (34) was numerically confirmed in the computer simulation of a glassy molecular liquid in Ref. [148].

More generally, relaxation in glassy systems occurs in well-separated time sectors [141]; it is then easy to imagine that each sector could be associated with an effective temperature [147]. A thermodynamic interpretation of effective temperatures has also been put forward, relating them to the concept of replica symmetry breaking [149]. Interestingly, the full-step or one-step replica symmetry breaking schemes needed to solve the static problem in these models have a counterpart as the FDR being a function or a number, respectively, in the aging regime. Moreover, we note that these modern concepts are related to, but make much more precise, older ideas of quasi-equilibrium and fictive temperatures in aging glasses [3].

Taken together, these results make the mean-field description of aging very appealing, and they nicely complement the mode-coupling/RFOT description of the equilibrium glass transition described above. Moreover, they have set the agenda for a large body of numerical and experimental work, as reviewed in [143]. In Fig. 16 we present recent numerical data obtained in an aging silica glass [150], presented in the form of a parametric response-correlation plot. The measured correlation functions are the self-part of the intermediate scattering functions defined in Eq. (5), while the conjugated response functions quantify the response of particle dis-

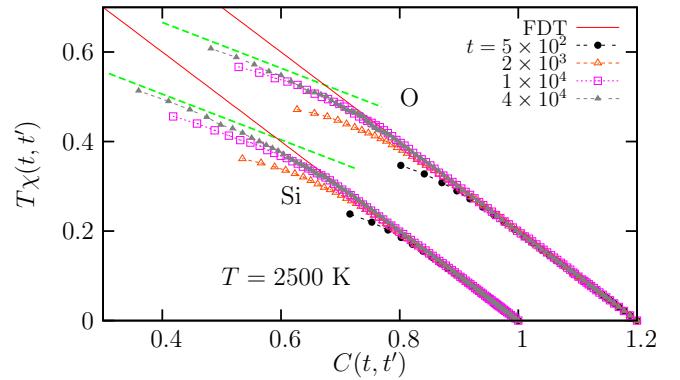


FIG. 16: Parametric correlation-response plots measured in the aging regime of a numerical model for a silica glass, SiO_2 [150]. The plots for both species smoothly converges towards a two-straight line plot of slope 1 at short times (large C values), and of slope $X^\infty \approx 0.51$ at large times (small values of C), yielding an effective temperature of about $T_{\text{eff}} = T/X^\infty \approx 4900$ K.

placements to a spatially modulated field conjugated to the density. Plots for silicon and oxygen atoms at different ages of the system are presented. They seem to smoothly converge towards a two-straight line plot, as obtained in mean-field models. Moreover, the second, non-trivial part of the plot is characterized by a slope that appears to be independent of the species, and of the wavevector chosen to quantify the dynamics, in agreement with the idea of a unique asymptotic value of the FDR, possibly related to a well-defined effective temperature.

D. Beyond mean-field

Despite successes such as shown in Fig. 16, the broader applicability of the mean-field scenario of aging dynamics remains unclear, however. While some experiments and simulations indeed seem to support the existence of well-behaved effective temperatures [151–153], other studies also reveal the limits of the mean-field scenario. Experiments have for instance reported anomalously large FDT violations associated with intermittent dynamics [154–157], while theoretical studies of model systems have also found non-monotonic or even negative response functions [158–161], and ill-defined or observable-dependent FDRs [162]. In principle, these discrepancies with mean-field predictions are to be expected, since there are many systems of physical interest in which the dynamics are not of mean-field type, displaying both activated processes and spatial heterogeneity.

It is thus an important task to understand from the theoretical point of view when the mean-field concept of an FDR-related effective temperature remains viable. However, studying theoretically the interplay between relevant dynamic lengthscales and thermally activated

dynamics in the non-equilibrium regime of disordered materials is clearly a challenging task. Nevertheless, this problem has been approached in different ways, as we briefly summarize in this subsection.

A first class of system that displays aging and spatial heterogeneity is given by coarsening systems. The paradigmatic situation is that of an Ising ferromagnetic model (with a transition at T_c) suddenly quenched in the ferromagnetic phase at time $t_w = 0$. For $t_w > 0$ domains of positive and negative magnetizations appear and slowly coarsen with time. The appearance of domains that grow with time proves the presence of both aging and heterogeneity in this situation.

The case where the quench is performed down to $T < T_c$ is well understood. The system becomes scale invariant [163], since the only relevant lengthscale is the growing domain size, $\ell(t_w)$. Correlation functions display aging, and scale invariance implies that $C(t, t_w) \sim f(\ell(t)/\ell(t_w))$. Response functions can be decomposed into two contributions [164, 165]: one part stems from the bulk of the domains and behaves as the equilibrium response, and a second one from the domain walls and becomes vanishingly small in the long time limit where $\ell(t_w) \rightarrow \infty$ and the density of domain walls vanishes. This implies that for coarsening systems in $d \geq 2$, one has $X^\infty = 0$, or equivalently an infinite effective temperature, $T_{\text{eff}} = \infty$. The case $d = 1$ is special because $T_c = 0$ and the response function remains dominated by the domain walls, which yields the non-trivial value $X^\infty = 1/2$ [166].

Another special case has retained attention. When the quench is performed at $T = T_c$, there is no more distinction between walls and domains and the above argument yielding $X^\infty = 0$ does not hold. Instead one studies the growth with time of critical fluctuations, with $\xi(t_w) \sim t_w^{1/z}$ the correlation length at time t_w , where z is the dynamic exponent. Both correlation and response functions become non-trivial at the critical point [167]. It proves useful in that case to consider the dynamics of the Fourier components of the magnetization fluctuations, $C_q(t, t_w) = \langle m_q(t)m_{-q}(t_w) \rangle$, and the conjugated response $R_q(t, t_w) = \frac{\delta \langle m_q(t) \rangle}{\delta h_{-q}(t_w)}$. From Eq. (29) a wavevector dependent FDR follows, $X_q(t, t_w)$, which has interesting properties [168, 169].

In dimension $d = 1$, it is possible to compute $X_q(t, t_w)$ exactly in the aging regime at $T = T_c = 0$. An interesting scaling form is found, and numerical simulations performed for $d > 1$ confirm its validity:

$$X_q(t, t_w) = \mathcal{X}(q^2 t_w), \quad (35)$$

where the scaling function $\mathcal{X}(x)$ is $\mathcal{X}(x \rightarrow \infty) \rightarrow 1$ at small lengthscale, $q\xi \gg 1$, and $\mathcal{X}(x \rightarrow 0) \rightarrow 1/2$ (in $d = 1$) at large distance, $q\xi \ll 1$; recall that for $z = 2$ in that case.

Contrary to mean-field systems where geometry played no role, here the presence of a growing correlation lengthscale plays a crucial role in the off-equilibrium regime

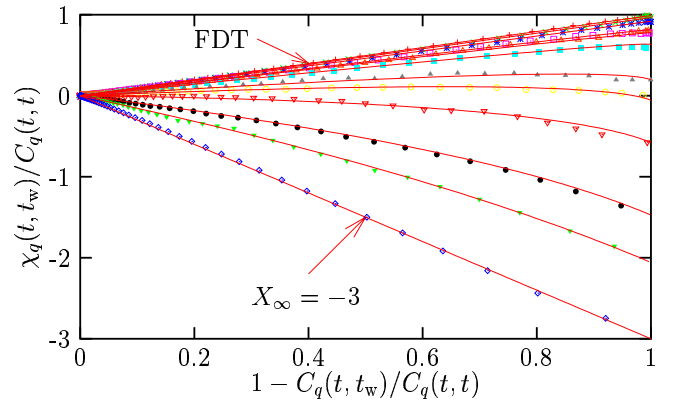


FIG. 17: Parametric response-correlation plots for the Fourier components of the mobility field in the $d = 3$ Fredrickson-Andersen model. Symbols are from simulations, lines from analytic calculations, and wavevectors decrease from top to bottom. The FDT is close to being satisfied at large q corresponding to local equilibrium. At larger distance deviations from the FDT are seen, with an asymptotic FDR which becomes negative. Finally, for energy fluctuations at $q = 0$ (bottom curve), the plot becomes a pure straight line of (negative!) slope -3 , as a result of thermally activated dynamics.

since $\xi(t_w)$ allows one to discriminate between fluctuations that satisfy the FDT at small lengthscale, $X_q \sim 1$, and those at large lengthscale which are still far from equilibrium, $0 < X_q \sim X^\infty < 1$. These studies suggest therefore that generalized fluctuation-dissipation relation in fact have a strong lengthscale dependence—a result which is not predicted by mean-field approaches.

Another interesting result is that the FDT violation for global observables (i.e. those at $q = 0$) takes a particularly simple form, since the introduction of a single number is sufficient, the FDR at zero wavevector, $X_{q=0}(t, t_w) \equiv X^\infty = 1/2$ (in $d = 1$). This universal quantity takes non-trivial values in higher dimension, e.g. $X^\infty \approx 0.34$ is measured in $d = 2$ [168]. This shows that the study of global rather than local quantities makes the measurement of X^∞ much easier. Finally, having a non-trivial value of X^∞ for global observables suggests that the possibility to define an effective temperature remains valid, but it has become a more complicated object, related to global fluctuations on large lengthscale.

Kinetically constrained spin models represent a second class of non-mean-field systems whose off-equilibrium has been thoroughly studied recently [104]. This is quite a natural thing to do since these systems have local, finite ranged interactions, and they combine the interesting features of being defined in terms of (effective) microscopic degrees of freedom, having local dynamical rules, and displaying thermally activated and heterogeneous dynamics.

The case of the Fredrickson-Andersen model, described in Sec. VII, has been studied in great detail [104], and we summarize the main results. Here, the relevant dynamic variables are the Fourier components of the mobility field, which also correspond in that case to the fluctuation-dissipation relation.

tuations of the energy density. Surprisingly, the structure of the generalized fluctuation-dissipation relation remains once more very simple. In particular, in dimension $d > 2$, one finds a scaling form similar to (35), $X_q(t, t_w) = \mathcal{X}(q^2 t_w)$, with a well-defined limit at large distance $X_{q=0}(t, t_w) \equiv X^\infty$. The deep analogy with critical Ising models stems from the fact that mobility defects in KCMs diffuse in a way similar to domain walls in coarsening Ising models. It is in fact by exploiting this analogy that analytic results are obtained in the aging regime of the Fredrickson-Andersen model [170].

There is however a major qualitative difference between the two families of model. The (big!) surprise lies in the sign of the asymptotic FDR, since calculations show that [171]

$$X^\infty = -3, \quad d > 2. \quad (36)$$

In dimension $d = 1$, one finds $X_{q=0}(t, t_w) = f(t/t_w)$ with $X_{q=0}(t \rightarrow \infty, t_w) = \frac{3\pi}{16-6\pi} \approx -3.307$. Numerical simulations confirm these calculations. In Fig. 17, we show such a comparison between simulations (symbols) and theory (lines) in the case of the $d = 3$ Fredrickson-Andersen model [171]. Fourier components of the mobility field yield parametric FD plots that follow scaling with the variable $q^2 t_w$, as a direct result of the presence of a growing lengthscale for dynamic heterogeneity, $\xi(t_w) \sim \sqrt{t_w}$. Again, generalized fluctuation-dissipation relations explicitly depend on the spatial lengthscale considered, unlike in mean-field studies. In Fig. 17, the limit $q = 0$ corresponding to global observables is also very interesting since the plot is a pure straight line, as in equilibrium. Unlike equilibrium, however, the slope is not 1 but -3 . A negative slope in this plot means a negative FDR, and therefore suggests a negative effective temperature, an very non-intuitive result at first sight.

Negative response functions in fact directly follows from the thermally activated nature of the dynamics of these models [171]. First, one should note that the global observable shown in Fig. 17 corresponds to fluctuations of the energy, $e(t_w)$, whose conjugated field is temperature. In the aging regime the system slowly drifts towards equilibrium. Microscopic moves result from thermally activated processes, corresponding to the local crossing of energy barriers. An infinitesimal change in temperature, $T \rightarrow T + \delta T$ with $\delta T > 0$, accelerates these barrier crossings and makes the relaxation dynamics faster. The energy response to a positive temperature pulse is therefore negative, $\delta e < 0$, which directly yields $\delta e / \delta T < 0$, which explains the negative sign of the FDR. This result does not hold in mean-field glasses, where thermal activation plays no role.

Finally, another scenario holds for local observables in some KCMs when kinetic constraints are stronger, such as the East model [104] or a bidimensional triangular plaquette model [172]. Here, relaxation is governed by a hierarchy of energy barriers that endow the systems with specific dynamic properties. In the aging regime following a quench, in particular, the hierarchy yields

an energy relaxation that arises in discrete steps which take place on very different timescales, reminiscent of the ‘time sectors’ encountered in mean-field spin glasses. Surprisingly, it is found that to each of these discrete relaxations one can associate a well-defined (positive) value of the fluctuation-dissipation ratio, again reminiscent of the dynamics of mean-field spin glass models. Therefore, even in models that are very far from the mean-field limit the physical picture of a slow relaxation taking place on multiple timescales with each timescale characterized by an effective temperature seems to have some validity.

E. Driven glassy materials

We have introduced aging phenomena with the argument that in a glass phase, the timescale to equilibrate becomes so long that the system always remembers its complete history. This is true in general, but one can wonder whether it is possible to invent a protocol where the material history could be erased, and the system ‘rejuvenated’ [173]. This concept has been known for decades in the field of polymer glasses, where complex thermo-mechanical histories are often used.

Let us consider an aging protocol where the system is quenched to low temperature at time $t_w = 0$, but the system is simultaneously forced by an external mechanical constraint. Experimentally one finds that a stationary state can be reached, which explicitly depends on the strength of the forcing: a system which is forced more strongly relaxes faster than a less solicited material, a phenomenon called ‘shear-thinning’. The material has therefore entered a driven steady state, where memory of its age is no longer present and dynamics has become stationary: aging is stopped.

Many studies of these driven glassy states have been performed in recent years. In the language of the jamming phase diagram in Fig. 4, these correspond to studies of the (Temperature, Load) plane for molecular liquids, or the (1/Density, Load) plane for colloidal systems. The former studies are relevant for the rheology of supercooled liquids and glasses, and the $T \ll T_g$ limit corresponds to studies of the plasticity of amorphous solids, a broad field in itself. In the colloidal world, such studies are also relevant for the newly-defined field of the rheology of ‘soft glassy materials’. These materials are (somewhat tautologically) defined as those for which the non-linear rheological behaviour is believed to result precisely from the competition between intrinsically slow relaxation processes and an external forcing [174]. It is believed that the rheology of dense colloidal suspensions, foams, emulsions, binary mixtures, or even biophysical systems are ruled by such a competition, quite a broad field of application indeed.

From the point of view of statmech modeling, soft glassy rheology can be naturally studied from the very same angles as the glass transition itself. As such there are many models [174, 175], mean-field spin glasses [81] and the re-

lated mode-coupling theory approach [82, 83] have been explicitly extended to include an external mechanical forcing. In all these cases, one finds that a driven steady state can be reached and aging is indeed expected to stop at a level that depends on the strength of the forcing. Many of the results obtained in aging systems about the properties of an effective temperature are also shown to apply in the driven case, as shown both theoretically [81] and numerically [176]. A most interesting aspect is that the broad relaxation spectra predicted to occur in glassy materials close to a glass transition directly translate into ‘anomalous’ laws both for the linear rheological behaviour (seen experimentally in the broad spectrum of elastic, $G'(\omega)$, and loss, $G''(\omega)$, moduli), and the non-linear rheological behaviour (a strong dependence of the viscosity η upon the shear rate $\dot{\gamma}$).

IX. FUTURE DIRECTIONS

The problem of the glass transition, already very exciting in itself, has ramifications well beyond the physics of supercooled liquids. Glassy systems figures among the even larger class of ‘complex systems’. These are formed by a set of interacting degrees of freedom that show an emergent behaviour: as a whole they exhibit properties not obvious from the properties of the individual parts. As a consequence the study of glass-formers as statistical mechanics model characterized by frustrated interactions is a fertile ground to develop new concepts and techniques that will likely be applied to other physical, and more generally, scientific situations.

An example, already cited in this review, are the recent progress obtained in computer science and information theory [5] using techniques originally developed for spin glasses and structural glasses. More progress is certainly expected in the future along these interdisciplinary routes. Concerning physics, glassiness is such an ubiquitous and, yet as we showed, rather poorly understood problem that many developments are very likely to take place in the next decade.

Instead of guessing future developments of the field

(and then very likely be proven wrong!) we prefer to list a few problems we would like to see solved in the next years.

- Are the jamming transitions of granular media and colloids related to the glass transition of supercooled liquids? If yes, what is the common physical mechanism behind the dramatic slowing down?
- Is the glass transition related to a true phase transition? If yes, a static or a dynamic one? A finite or zero temperature one?
- Do RFOT, defects models, or frustration-based theory form the correct starting points of ‘the’ theory of the glass transition?
- What is the correct physical picture for the low temperature phase of glass-forming liquids and spin glasses?
- Are there general principles governing off-equilibrium equilibrium dynamics, and in particular aging and sheared materials?
- Do non-disordered, finite-dimensional, finite-range statmech model exist that display a thermodynamically stable amorphous phase at low temperature?

Finally, notice that we did not discuss possible interplays between glassiness and quantum fluctuations. This is a very fascinating topic. Quantum glassiness, and more generally, slow quantum dynamics are research subjects which are still in their infancies but that will likely undergo exciting developments in the near future.

Acknowledgments

We thank C. Marchetti for inviting us to write this review and the collaborators who worked with us on glass physics. Our work is supported by ANR Grants CHEF, TSANET and DYNHET.

-
- [1] C. A. Angell, *Science* **267**, 1924 (1995).
 - [2] P.G. Debenedetti and F. H. Stillinger, *Nature* **410**, 259 (2001).
 - [3] L. C. E. Struik, *Physical aging in amorphous polymers and other materials* (Elsevier, Amsterdam, 1978).
 - [4] *Spin glasses and random fields*, Ed.: A. P. Young (World Scientific, Singapore, 1998).
 - [5] *Complex systems*, Eds.: M. Mézard, J.-P. Bouchaud, and J. Dalibard (Springer, Berlin, 2007).
 - [6] H. Bässler, *Phys. Rev. Lett.* **58**, 767 (1987).
 - [7] R. Richert and C. A. Angell, *J. Chem. Phys.* **108**, 9016 (1998).
 - [8] A. W. Kauzmann, *Chem. Rev.* **43**, 219 (1948)
 - [9] M. Goldstein, *J. Chem. Phys.* **51**, 3728 (1969)
 - [10] P. G. Debenedetti, *Metastable liquids* (Princeton University Press, Princeton, 1996)
 - [11] See however N. Menon and S. R. Nagel *Phys. Rev. Lett.* **74**, 1230 (1995); L. A. Fernández, V. Martin-Mayor, and P. Verrocchio *Phys. Rev. E* **73**, 020501 (2006); Refs [96].
 - [12] J. Wuttke, W. Petry, and S. Pouget, *J. Chem. Phys.* **105**, 5177 (1996).
 - [13] K. Binder and W. Kob, *Glassy materials and disordered solids* (World Scientific, Singapore, 2005).
 - [14] L.C. Pardo, P. Lunkenheimer, A. Loidl, *Phys. Rev. E* **76**, 030502(R) (2007).
 - [15] R. G. Larson, *The Structure and Rheology of Complex*

- Fluids* (Oxford University Press, New York, 1999).
- [16] P. N. Pusey and W. van Meegen, *Nature* **320**, 340 (1986).
- [17] Z. Cheng, J., P. M. Chaikin, S. Phan, and W. B. Russel, *Phys. Rev. E* **65**, 041405 (2002).
- [18] W. K. Kegel and A. van Blaaderen, *Science* **287**, 290 (2000).
- [19] E. Weeks, J. C. Crocker, A. C. Levitt, A. Schofield, and D. A. Weitz, *Science* **287**, 627 (2000).
- [20] L. Cipelletti, L. Ramos, *Journal of Physics: Condensed Matter* **17** (2005) R253.
- [21] H. M. Jaeger, S. R. Nagel, and R. P. Behringer, *Rev. Mod. Phys.* **68**, 1259 (1996).
- [22] G. D'Anna, G. Gremaud, *Nature* **413**, 407 (2001).
- [23] G. Marty and O. Dauchot, *Phys. Rev. Lett.* **94**, 015701 (2005).
- [24] A. S. Keys, A. R. Abate, S. C. Glotzer, and D. J. Durian, *Nat. Phys.* **3**, 260 (2007).
- [25] A. J. Liu and S. R. Nagel, *Nature* **396**, 21 (1998).
- [26] F. Krzakala, A. Montanari, F. Ricci-Tersenghi, G. Semerjian, and L. Zdeborová, *PNAS* (2007) **104** 10318.
- [27] E. Vidal Russell and N. E. Israeloff, *Nature* **408**, 695 (2000).
- [28] A. N. Adhikari, N. A. Capurso, and D. Bingemann, *J. Chem. Phys.* **127**, 114508 (2007).
- [29] M. Allen and D. Tildesley, *Computer Simulation of Liquids* (Oxford University Press, Oxford, 1987).
- [30] J. Horbach and W. Kob, *Phys. Rev. E* **64**, 041503 (2001).
- [31] W. Götze, *J. Phys.: Condens. Matter* **11**, A1 (1999).
- [32] T. Gleim, W. Kob, and K. Binder, *Phys. Rev. Lett.* **81**, 4404 (1998).
- [33] G. Szamel and E. Flenner, *Europhys. Lett.* **67**, 779 (2004).
- [34] L. Berthier and W. Kob, *J. Phys.: Condens. Matter* **19**, 205130 (2007).
- [35] L. Berthier, G. Biroli, J.-P. Bouchaud, W. Kob, K. Miyazaki, and D. R. Reichman, *J. Chem. Phys.* **126**, 184503 (2007).
- [36] L. Berthier, G. Biroli, J.-P. Bouchaud, W. Kob, K. Miyazaki, and D. R. Reichman, *J. Chem. Phys.* **126**, 184504 (2007).
- [37] J. P. Garrahan, D. Chandler, *Phys. Rev. Lett.* **89**, 035704 (2002).
- [38] M. M. Hurley and P. Harrowell, *Phys. Rev. E* **52**, 1694 (1995).
- [39] M. D. Ediger, *Annu. Rev. Phys. Chem.* **51**, 99 (2000).
- [40] W. Kob, C. Donati, S. J. Plimpton, P. H. Poole, and S. C. Glotzer, *Phys. Rev. Lett.* **79**, 2827 (1997).
- [41] P. Chaudhuri, L. Berthier, and W. Kob, *Phys. Rev. Lett.* **99**, 060604 (2007).
- [42] J. P. Hansen and I. R. McDonald, *Theory of Simple Liquids* (Academic, London, 1986).
- [43] M. K. Mapes, S. F. Swallen, and M. D. Ediger, *J. Chem. Phys.* **124**, 054710 (2006).
- [44] G. Tarjus and D. Kivelson, *J. Chem. Phys.* **103**, 3071 (1995).
- [45] Y. Jung, J.P. Garrahan, and D. Chandler, *Phys. Rev. E* **69**, 061205 (2004).
- [46] U. Tracht, M. Wilhelm, A. Heuer, H. Feng, K. Schmidt-Rohr, and H. W. Spiess, *Phys. Rev. Lett.* **81**, 2727 (1998); S. A. Reinsberg, X. H. Qiu, M. Wilhelm, H. W. Spiess, M. D. Ediger, *J. Chem. Phys.* **114**, 7299 (2001).
- [47] S. Franz and G. Parisi, *J. Phys.: Condens. Matter* **12**, 6335 (2000).
- [48] C. Toninelli, M. Wyart, L. Berthier, G. Biroli, and J.-P. Bouchaud, *Phys. Rev. E* **71**, 041505 (2005).
- [49] R. Yamamoto and A. Onuki, *Phys. Rev. E* **58**, 3515 (1998).
- [50] S. Franz, C. Donati, G. Parisi, and S. C. Glotzer, *Philos. Mag. B* **79**, 1827 (1999).
- [51] C. Bennemann, C. Donati, J. Baschnagel, and S. C. Glotzer, *Nature* **399**, 246 (1999); N. Laceyvic, F. W. Starr, T. B. Schroder, and S. C. Glotzer, *J. Chem. Phys.* **119**, 7372 (2003).
- [52] L. Berthier, *Phys. Rev. E* **69**, 020201(R) (2004).
- [53] M. Vogel and S. C. Glotzer, *Phys. Rev. E* **70**, 061504 (2004).
- [54] L. Berthier, *Phys. Rev. E* **76**, 011507 (2007).
- [55] O. Dauchot, G. Marty, and G. Biroli, *Phys. Rev. Lett.* **95**, 265701 (2005).
- [56] E. R. Weeks, J. C. Crocker, and D. A. Weitz, *J. Phys.: Condens. Matter* **19**, 205131 (2007).
- [57] L. Berthier, G. Biroli, J.-P. Bouchaud, L. Cipelletti, D. El Masri, D. L'Hôte, F. Ladieu, and M. Pierno, *Science* **310**, 1797 (2005).
- [58] C. Dalle-Ferrier, C. Thibierge, C. Alba-Simionesco, L. Berthier, G. Biroli, J.-P. Bouchaud, F. Ladieu, D. L'Hôte, and G. Tarjus *Phys. Rev. E* **76**, 041510 (2007).
- [59] X. Y. Xia and P. G. Wolynes, *Proc. Natl. Acad. Sci. U.S.A.* **97**, 2990 (2000).
- [60] J. P. Garrahan and D. Chandler, *Proc. Natl. Acad. Sc U.S.A.* **100**, 9710 (2003).
- [61] G. Tarjus, S. A. Kivelson, Z. Nussinov, and P. Viot, *J. Phys.: Condens. Matter* **17**, R1143 (2005).
- [62] C. Donati, J. Douglas, W. Kob, S. J. Plimpton, P. H. Poole, and S. C. Glotzer, *Phys. Rev. Lett.* **80**, 2338 (1998).
- [63] G. A. Appignanesi, J. A. Rodriguez Fris, R. A. Montani, and W. Kob, *Phys. Rev. Lett.* **96**, 057801 (2006).
- [64] G. Adam and J. H. Gibbs, *J. Chem. Phys.* **43**, 139 (1958).
- [65] M. Mézard, G. Parisi, and M. Virasoro, *Spin Glass Theory and Beyond* (World Scientific, Singapore, 1988).
- [66] T. R. Kirkpatrick and D. Thirumalai, *Phys. Rev. Lett.* **58**, 2091 (1987); T. R. Kirkpatrick and P. G. Wolynes, *Phys. Rev. A* **35**, 3072 (1987).
- [67] G. Biroli and M. Mézard, *Phys. Rev. Lett.* **88**, 025501 (2001).
- [68] D. R. Nelson, *Defects and Geometry in Condensed Matter Physics* (Cambridge University Press, Cambridge, 2002).
- [69] G. D. McCullagh, D. Cellai, A. Lawlor, and K. A. Dawson, *Phys. Rev. E* **71**, 030102 (2005).
- [70] O. Rivoire, G. Biroli, O. C. Martin, M. Mézard, *Eur. Phys. J. B* **37**, 55 (2004).
- [71] D. J. Gross and M. Mézard, *Nucl. Phys. B* **240**, 431 (1984).
- [72] R. Monasson, *Phys. Rev. Lett.* **75**, 2847 (1995).
- [73] T. Castellani, A. Cavagna, *Lecture notes of the school: "Unifying Concepts in Glassy Physics III"*, Bangalore, June 2004, *J. Stat. Mech.* (2005) P05012
- [74] L. F. Cugliandolo in Ref. [75].
- [75] *Slow relaxations and nonequilibrium dynamics in condensed matter*, Eds: J.-L. Barrat, J. Dalibard, M. Feigelman, J. Kurchan (Springer, Berlin, 2003).
- [76] E. Leutheusser, *Phys. Rev. A* **29**, 2765 (1984).
- [77] U. Bengtzelius, W. Götze, A. Sjölander, *J. Phys. C* **17**, 5915 (1984).

- [78] S. P. Das and G. F. Mazenko, Phys. Rev. A **34**, 2265 (1986).
- [79] G. Biroli and J. P. Bouchaud, Europhys. Lett. **67**, 21 (2004).
- [80] G. Biroli, J.-P. Bouchaud, K. Miyazaki, and D. R. Reichman, Phys. Rev. Lett. **97**, 195701 (2006).
- [81] L. Berthier, J.-L. Barrat, and J. Kurchan, Phys. Rev. E **61**, 5464 (2000).
- [82] K. Miyazaki and D. R. Reichman, Phys. Rev. E **66**, 050501(R) (2002).
- [83] M. Fuchs and M. E. Cates, Phys. Rev. Lett. **89**, 248304 (2002).
- [84] T. R. Kirkpatrick, D. Thirumalai, and P. G. Wolynes, Phys. Rev. A **40**, 1045 (1989).
- [85] J.-P. Bouchaud and G. Biroli, J. Chem. Phys. **121**, 7347 (2004).
- [86] M. Dzero, J. Schmalian, and P. G. Wolynes, Phys. Rev. B **72**, 100201 (2005).
- [87] S. Franz, J. Stat. Mech. P04001 (2005); Europhys. Lett. **73**, 492 (2006);
- [88] C. A. Angell, J. Res. NIST **102**, 171 (1997).
- [89] I. Hodge, J. Res. NIST **102**, 195 (1997).
- [90] G. P. Johari, J. Chem. Phys. **112**, 8958 (2000).
- [91] M. Mézard and G. Parisi, Phys. Rev. Lett. **82**, 747 (1999).
- [92] G. Parisi and F. Zamponi, J. Chem. Phys. **123**, 144501 (2005).
- [93] F. Thalmann, J. Chem. Phys. **116**, 3378 (2002).
- [94] B. Coluzzi and P. Verrocchio, J. Chem. Phys. **116**, 3789 (2002).
- [95] M. Nauroth and W. Kob, Phys. Rev. E **55**, 657 (1997).
- [96] A. Cavagna, T. S. Grigera, and P. Verrocchio, Phys. Rev. Lett. **98**, 187801 (2007).
- [97] W. Kob and H. C. Andersen, Phys. Rev. E **48**, 4364 (1993).
- [98] F. Ritort and P. Sollich, Adv. Phys. **52**, 219 (2003).
- [99] S. Franz, R. Mulet, and G. Parisi, Phys. Rev. E **65**, 021506 (2002).
- [100] C. Toninelli, G. Biroli, and D. S. Fisher, Phys. Rev. Lett. **92**, 185504 (2004).
- [101] A. C. Pan, J. P. Garrahan, D. Chandler, Phys. Rev. E **72**, 041106 (2005).
- [102] S. H. Glarum, J. Chem. Phys. **33**, 639 (1960).
- [103] G. H. Fredrickson and H. C. Andersen, Phys. Rev. Lett. **53**, 1244 (1984).
- [104] S. Léonard, P. Mayer, P. Sollich, L. Berthier, and J. P. Garrahan, J. Stat. Mech. P07017 (2007).
- [105] M. H. Cohen and G. S. Grest, Phys. Rev. B **26**, 6313 (1982).
- [106] G. H. Fredrickson and S. A. Brawer, J. Chem. Phys. **84**, 3351 (1986).
- [107] S. Butler and P. Harrowell, J. Chem. Phys. **95**, 4454 (1991); J. Chem. Phys. **95**, 4466 (1991).
- [108] C. Toninelli, G. Biroli, and D. S. Fisher, Phys. Rev. Lett. **96**, 035702 (2006).
- [109] S. Whitelam, L. Berthier, and J.P. Garrahan, Phys. Rev. E **71**, 026128 (2005).
- [110] L. Berthier and J.P. Garrahan, J. Phys. Chem. B **109**, 3578 (2005).
- [111] R. L. Jack, P. Mayer, and P. Sollich, J. Stat. Mech.: Theory Exp. P03006 (2006).
- [112] L. Berthier, D. Chandler, and J.P. Garrahan, Europhys. Lett. **69**, 320 (2005).
- [113] D. Chandler, J. P. Garrahan, R. L. Jack, L. Maibaum and A.C. Pan, Phys. Rev. E **74**, 051501 (2006).
- [114] S. Whitelam, L. Berthier, and J. P. Garrahan, Phys. Rev. Lett. **92**, 185705 (2004).
- [115] M. T. Downton and M. P. Kennett, Phys. Rev. E **76**, 031502 (2007).
- [116] J. P. Garrahan, J. Phys. Condens. Matter **14**, 1571 (2002).
- [117] R. L. Jack, L. Berthier, and J. P. Garrahan, Phys. Rev. E **72**, 016103 (2005).
- [118] A. Lipowski, D. Johnston, D. Espriu, Phys. Rev. E **62**, 3404 (2000).
- [119] J. P. Sethna, J. D. Shore, and M. Huang, Phys. Rev. B **44**, 4943 (1991).
- [120] G. Biroli, J.-P. Bouchaud, and G. Tarjus, J. Chem. Phys. **123**, 044510 (2005).
- [121] M. Sellitto, G. Biroli, C. Toninelli Europhys. Lett. **69** 496 (2005).
- [122] L. Berthier and J. P. Garrahan, J. Chem. Phys. **119**, 4367 (2003).
- [123] S. Whitelam and J. P. Garrahan, J. Phys. Chem. B **108**, 6611 (2004).
- [124] R. L. Jack and J. P. Garrahan, J. Chem. Phys. **123**, 164508 (2005).
- [125] F. C. Franck, Proc. R. Soc. London **215**, 43 (1952).
- [126] D. Kivelson, S. A. Kivelson, X.-L. Zhao, Z. Nussinov, and G. Tarjus, Physica A **219**, 27 (1995).
- [127] D. Coslovich and G. Pastore, J. Chem. Phys. **127**, 124504 (2007).
- [128] J. P. Bouchaud, J. Phys. I France **2**, 1705 (1992).
- [129] A. J. Bray and M.A. Moore, J. Phys. C **17**, L463 (1984); and in *Heidelberg Colloquium on Glassy Dynamics*, Eds.: J. L. van Hemmen and I. Morgenstern, Lectures Notes in Physics Vol. 275 (Springer, Berlin, 1987).
- [130] D. S. Fisher and D. A. Huse, Phys. Rev. Lett. **56**, 1601 (1986).
- [131] J. Kisker, L. Santen, M. Schreckenberg, and H. Rieger, Phys. Rev. B **53**, 6418 (1996).
- [132] P. Réfrégier, E. Vincent, J. Hammann, and M. Ocio, J. Phys. France **48**, 1533 (1987).
- [133] L. Berthier and A. P. Young, Phys. Rev. B **71**, 214429 (2005).
- [134] L. Berthier, V. Viasnoff, O. White, V. Orlyanchik, and F. Krzakala, in Ref. [75]
- [135] J.-P. Bouchaud, V. Dupuis, J. Hammann, and E. Vincent, Phys. Rev. B **65**, 024439 (2001).
- [136] L. Berthier and J.-P. Bouchaud, Phys. Rev. B **66**, 054404 (2002).
- [137] F. Bert, V. Dupuis, E. Vincent, J. Hammann, and J.-P. Bouchaud, Phys. Rev. Lett. **92**, 167203 (2004).
- [138] A. J. Bray and M. A. Moore, Phys. Rev. Lett. **58**, 57 (1987).
- [139] P. E. Jönsson, R. Mathieu, P. Nordblad, H. Yoshino, H. Aruga Katori, and A. Ito Phys. Rev. B **70**, 174402 (2004).
- [140] L. F. Cugliandolo and J. Kurchan, Phys. Rev. Lett. **71**, 173 (1993).
- [141] L. F. Cugliandolo and J. Kurchan, J. Phys. A **27**, 5749 (1994).
- [142] S. Franz and M. Mézard, Europhys. Lett. **26** 209 (1994).
- [143] A. Crisanti and F. Ritort, J. Phys. A **36** R181 (2003).
- [144] J. Kurchan and L. Laloux, J. Phys. A **29**, 1929 (1996).
- [145] L. F. Cugliandolo, J. Kurchan, and L. Peliti, Phys. Rev. E **55**, 3898 (1997).
- [146] S. Franz, M.A. Virasoro J. Phys. A **33** (2000) 891.

- [147] J. Kurchan, *Nature* **433**, 222 (2005).
- [148] L. Berthier and J.-L. Barrat, *Phys. Rev. Lett.* **89**, 095702 (2002).
- [149] S. Franz, M. Mézard, G. Parisi, and L. Peliti, *Phys. Rev. Lett.* **81**, 1758 (1998).
- [150] L. Berthier, *Phys. Rev. Lett.* **98**, 220601 (2007).
- [151] T. S. Grigera and N. E. Israeloff, *Phys. Rev. Lett.* **83**, 5038 (1999).
- [152] B. Abou and F. Gallet, *Phys. Rev. Lett.* **93**, 160603 (2004).
- [153] P. Wang, C. M. Song, and H. A. Makse, *Nat. Phys.* **2**, 526 (2006).
- [154] L. Bellon, S. Ciliberto, and C. Laroche, *Europhys. Lett.* **53**, 511 (2001).
- [155] L. Bellon and S. Ciliberto, *Physica D* **168**, 325 (2002).
- [156] L. Buisson, L. Bellon, and S. Ciliberto, *J. Phys.: Condens. Matter* **15**, S1163 (2003).
- [157] L. Buisson, S. Ciliberto, and A. Garcimartin, *Europhys. Lett.* **63**, 603 (2003).
- [158] P. Viot, J. Talbot, and G. Tarjus, *Fractals* **11**, 185 (2003).
- [159] M. Nicodemi, *Phys. Rev. Lett.* **82**, 3734 (1999).
- [160] F. Krzakala, *Phys. Rev. Lett.* **94**, 077204 (2005).
- [161] M. Depken and R. Stinchcombe, *Phys. Rev. E* **71**, 065102 (2005).
- [162] S. Fielding and P. Sollich, *Phys. Rev. Lett.* **88**, 050603 (2002).
- [163] A. J. Bray, *Adv. Phys.* **43**, 357 (1994).
- [164] A. Barrat, *Phys. Rev. E* **57**, 3629 (1998).
- [165] L. Berthier, J.-L. Barrat and J. Kurchan, *Eur. Phys. J. B* **11**, 635 (1999).
- [166] C. Godrèche and J.-M. Luck, *J. Phys. A* **33**, 1151 (2000); ‘ E. Lippiello and M. Zannetti, *Phys. Rev. E* **61**, 3369 (2000).
- [167] C. Godrèche and J.-M. Luck, *J. Phys. A* **33**, 9141 (2000).
- [168] P. Mayer, L. Berthier, J.P. Garrahan, and P. Sollich, *Phys. Rev. E* **68**, 016116 (2003)
- [169] P. Calabrese and A. Gambassi, *J. Phys. A* **38**, R133 (2005).
- [170] P. Mayer and P. Sollich, *J. Phys. A* **40**, 5823 (2007).
- [171] P. Mayer, S. Léonard, L. Berthier, J. P. Garrahan, and P. Sollich, *Phys. Rev. Lett.* **96**, 030602 (2006).
- [172] R. L. Jack, L. Berthier, and J. P. Garrahan, *J. Stat. Mech.* P12005 (2006).
- [173] G. B. McKenna and A. J. Kovacs, *Polym. Eng. Sci.* **24**, 1131 (1984).
- [174] P. Sollich, F. Lequeux, P. Hebraud, and M. E. Cates, *Phys. Rev. Lett.* **78**, 2020 (1997)
- [175] P. Sollich, *Phys. Rev. E* **58**, 738 (1998).
- [176] L. Berthier and J.-L. Barrat, *J. Chem. Phys.* **116**, 6228 (2002).
- [177] The terminology ‘strong’ and ‘fragile’ is not related to the mechanical properties of the glass but to the evolution of the short-range order close to T_g . Strong liquids, such as SiO_2 , have a locally tetrahedric structure which persists both below and above the glass transition contrary to fragile liquids whose short-range amorphous structure disappears rapidly upon heating above T_g .
- [178] The decrease at long times constitutes a major difference with spin glasses. In a spin glass, χ_4 would be a monotonically increasing function of time whose long-time limit coincides with the static spin glass susceptibility. Physically, the difference is that spin glasses develop long-range static amorphous order while structural glasses do not or, at least, in a different and more subtle way.
- [179] In order to have a well-defined thermodynamics, Bethe lattices are generated as random graphs with fixed connectivity, also called random regular graphs.
- [180] There is of course no crystal state in disordered systems such as in Eq. (14). In the case of lattice glass models, there is a crystal phase but it can disappear depending whether the Bethe lattice is a Cayley tree or a random regular graph.
- [181] A critical (different) behaviour is expected and predicted for models having a transition [108].
- [182] This type of plaquette models, and other spin models, were introduced originally [118, 119] to show how ultra-slow glassy dynamics can emerge because of growing free energy barriers.
- [183] Most KCMs do not have a finite temperature dynamical transition and the ones displaying a transition have critical properties different from MCT.